

ELECTRIC DRIVE OPTIMISATION

CHONG CHEE KANG

**UNIVERSITI SAINS MALAYSIA
2012**

ELECTRIC DRIVE OPTIMISATION

By:

CHONG CHEE KANG

(Matrix no: 102449)

Supervisor:

Prof. Horizon Walker Gitano-Briggs

June 2012

This dissertation is submitted to
Universiti Sains Malaysia
As partial fulfillment of the requirement to graduate with honors degree in
BACHELOR OF ENGINEERING (MECHANICAL ENGINEERING)



School of Mechanical Engineering
Engineering Campus
Universiti Sains Malaysia

ACKNOWLEDGEMENTS

CONTENTS

Acknowledgements	ii
Contents	iii
List of Tables	vi
List of Figures	vii
List of Equations	ix
List of Abbreviations	x
List of Symbols	xi
Abstrak	xii
Abstract	xiii

CHAPTER 1 – INTRODUCTION

1.1 Background	1
1.2 Problem Statement	4
1.3 Objectives	6
1.4 Scope of Research	6
1.5 Research Approach	7
1.6 Summary	7

CHAPTER 2 – LITERATURE REVIEW

2.1 Introduction	9
2.2 Torque Ripple	9
2.3 Driving Strategy	11
2.4 Summary	14

CHAPTER 3 – METHODOLOGY

3.1	Introduction	15
3.2	Signal Identification	15
3.3	Measurement System.....	19
3.4	Vehicle Simulation	23
3.4.1	Track	23
3.4.2	Electric Motor	24
3.4.3	Air Drag Force	26
3.4.4	Rolling Resistance	26
3.4.5	Slope	26
3.4.6	Vehicle Acceleration	27
3.4.7	Combine Mathematical Model	27
3.5	Summary	28

CHAPTER 4 – RESULT AND DISCUSSION

4.1	Introduction	29
4.2	Signal Identification	29
4.3	Measurement System.....	30
4.4	Vehicle Simulation	30
4.5	Strategies	36
4.5.1	Preset Strategy 1	36
4.5.2	Preset Strategy 2	39
4.5.3	Preset Strategy 3	42
4.5.4	Comparison Between Strategies.....	45
4.6	Summary	46

CHAPTER 5 – CONCLUSION

References	50
------------------	----

APPENDICES	52
APPENDIX A – SCHEMATIC	53

LIST OF TABLES

	Page	
Table 4.1	Parameters for building the electric vehicle model	31
Table 4.2	Main result for "Full Throttle Everywhere"	33
Table 4.3	Main result for "Preset Strategy 1"	37
Table 4.4	Main result for "Preset Strategy 2"	41
Table 4.5	Main result for "Preset Strategy 3"	43

LIST OF FIGURES

	Page
Figure 1.1	Hall effect sensors signal, back emf, output torque and phase current (Yedamale, 2003) 3
Figure 1.2	The phase current and torque during an alternating comutation event (Salah et al., 2011) 5
Figure 2.1	Supervision Support System hardware configuration schematic (Shimizu et al., 1998) 12
Figure 2.2	Flowchart of the Cruising Simulation (Shimizu et al., 1998) 13
Figure 3.1	Hall effect sensor square wave signal (Point, 1999) 17
Figure 3.2	Circuit of hall effect sensor (Point, 1999) 17
Figure 3.3	16 pins controller circuit output 18
Figure 3.4	8 pins hall effect sensor I/O 19
Figure 3.5	Voltage Divider 21
Figure 3.6	Voltage Divider for negative voltage 22
Figure 3.7	Track gradient of Sepang North Track 24
Figure 3.8	Torque and power output curve for KLD D1064R (Technologies, 2010) 25
Figure 4.1	Vehicle parameter for initializing the vehicle model 31
Figure 4.2	Choosing the motor model 32
Figure 4.3	Choosing the track model 33
Figure 4.4	Setting the displacement interval for iteration 34
Figure 4.5	Graph of speed and gradient versus displacement for "full throttle everywhere" 34
Figure 4.6	Graph of power and gradient versus displacement for "full throttle everywhere" 35

Figure 4.7	Graph of air drag versus displacement for "full throttle everywhere"	35
Figure 4.8	Graph of Speed and Gradient versus displacement for "Preset Strategy 1"	37
Figure 4.9	Graph of Power and Gradient versus displacement for "Preset Strategy 1"	38
Figure 4.10	Graph of air drag versus displacement for "Preset Strategy 1"	38
Figure 4.11	Graph of Speed and Gradient versus displacement for "Preset Strategy 2"	39
Figure 4.12	Graph of Power and Gradient versus displacement for "Preset Strategy 2"	40
Figure 4.13	Graph of air drag versus displacement for "Preset Strategy 2"	41
Figure 4.14	Graph of Speed and Gradient versus displacement for "Preset Strategy 3"	43
Figure 4.15	Graph of Power and Gradient versus displacement for "Preset Strategy 3"	44
Figure 4.16	Graph of air drag versus displacement for "Preset Strategy 3"	44
Figure 4.17	Graph of power output versus displacement for various strategy	45
Figure 4.18	Graph of energy consumption for each strategy	46
Figure 4.19	Graph of vehicle mileage for each strategy	47
Figure 4.20	Graph of lap time for each strategy	47
Figure 4.21	Graph of drag torque versus displacement for each strategy	48

LIST OF EQUATIONS

	Page
3.1 Wheel speed for direct drive based on hall effect sensor signal, wheel diameter and PMBLDC number of poles	16
3.2 Power Input.....	20
3.3 Voltage Divider.....	21
3.4 Voltage Divider for negative voltage	21
3.5 Mathematical model for the torque of the electric motor	25
3.6 Relationship between power output, torque and rotational speed	25
3.7 Air drag force	26
3.8 Rolling resistance	26
3.9 Uphill/downhill force	26
3.10 Newton's Second Law of Motion	27
3.11 Combined mathematical model for vehicle dynamics	27
3.12 Acceleration/Deceleration of the electric vehicle	27
4.1 Relationship between the simulated vehicle mileage and real vehicle mileage.....	46

LIST OF ABBREVIATIONS

AC Alternating Current

BLDC Brushless DC

DC Direct Current

I/O Input Output

PMBLDC Permanent Magnet Brushless DC

PWM Pulse Width Modulation

SOC State of Charge

LIST OF SYMBOLS

lim limit

ABSTRAK

Abstrak versi bahasa melayu

ELECTRIC DRIVE OPTIMISATION

ABSTRACT

English version of the abstract

CHAPTER 1

INTRODUCTION

1.1 Background

Electric motor can be classified into two major categories which are the DC electric motor and AC electric motor. An AC motor is an electric motor driven by alternating current whereas a DC motor is driven by direct current. There are various types of AC motor which includes induction motor, synchronous motor, eddy current motor and etc. The DC electric motor includes permanent magnet brushed motor, permanent magnet brushless motor, switched reluctance motor and etc.

Electric motor is used in many application which includes in machine for driving the pulley and belts, the conveyor belt, in drilling and lathe machine. Apart from the heavy industry, electric motor is used in home appliances for powering the washing machine, fan, blower of air-conditioner and blender machine. Moreover, electric motor is used in automobile industry as the starter motor for firing up the internal combustion engine of cars and trucks and last but not least, as the drive train for electric vehicle.

The PMBLDC is a synchronous motor. In other words, the frequency of the magnetic field generated at the stator and the rotor is the same. PMBLDC comes in single-phase, 2-phase and 3-phase configuration. The 3-phase configuration is the most popular among the three. There are basically two major components inside a PMBLDC motor which is the stator and the rotor. The stator of a PMBLDC motor is made up of a series of laminated steel with wire windings around it. The rotor is build up of permanent magnet that has at least 2 poles.

Unlike brushed motor, PMBLDC does not have brushes for comutation, instead a controller is needed for controlling the rotation of the PMBLDC by sending out AC

signal to the PMBLDC. There are two types of AC signal sending to the PMBLDC for controlling the motor which are the Trapezoidal type and the Sinusoidal type which depends on the winding of the stator.

In order for the controller to send out the correct signal, the position of the rotor must be sent to the controller so that a sequence of AC signal can be generated which energized the winding of the stator for rotating the motor. Hall effect sensors is used as the rotor position detection sensor which has an analog signal output. When the magnetic field is detected by the hall effect sensor, the voltage output will be changes from lowest to the highest or vice versa depending on the circuit configuration. Normally there are three hall effect sensor mounted on the stator of PMBLDC motor which are 60° or 120° apart depending on the number of poles and the comutation sequence required.

Figure 1.1 shows the hall effect sensors signal for a 2 pole PMBLDC motor, the back emf, the phase current and the output torque. As shown in the figure, there are 3 hall effect sensors with labels A, B and C respectively, sensor A is leading sensor B by 60° and sensor B is leading sensor C by 60° .

Ideally, the phase current should behave as a digital square wave signal where the current rises and drops immediately. But in real world, the current would take some time to rises from zero to maximum/minimum. Hence, the torque produced would behave as a series of ripple instead of a constant output torque.

In this project, a PMBLDC hub motor is used as the sole powertrain of a electric vehicle. The electric vehicle will be used for participating in the Shell Eco-Marathon. It is a competition where teams compete for building the greatest mileage vehicle. The competition requires the participating teams to build their own car for the categories they are participating(for example, the urban concept category or the prototype category). For our case, a four-wheel electric vehicle is built for participation in urban concept category. The vehicle will be driven around a race track, which is the Sepang International Track, North Track for year 2012 for four laps with 10 seconds of stop

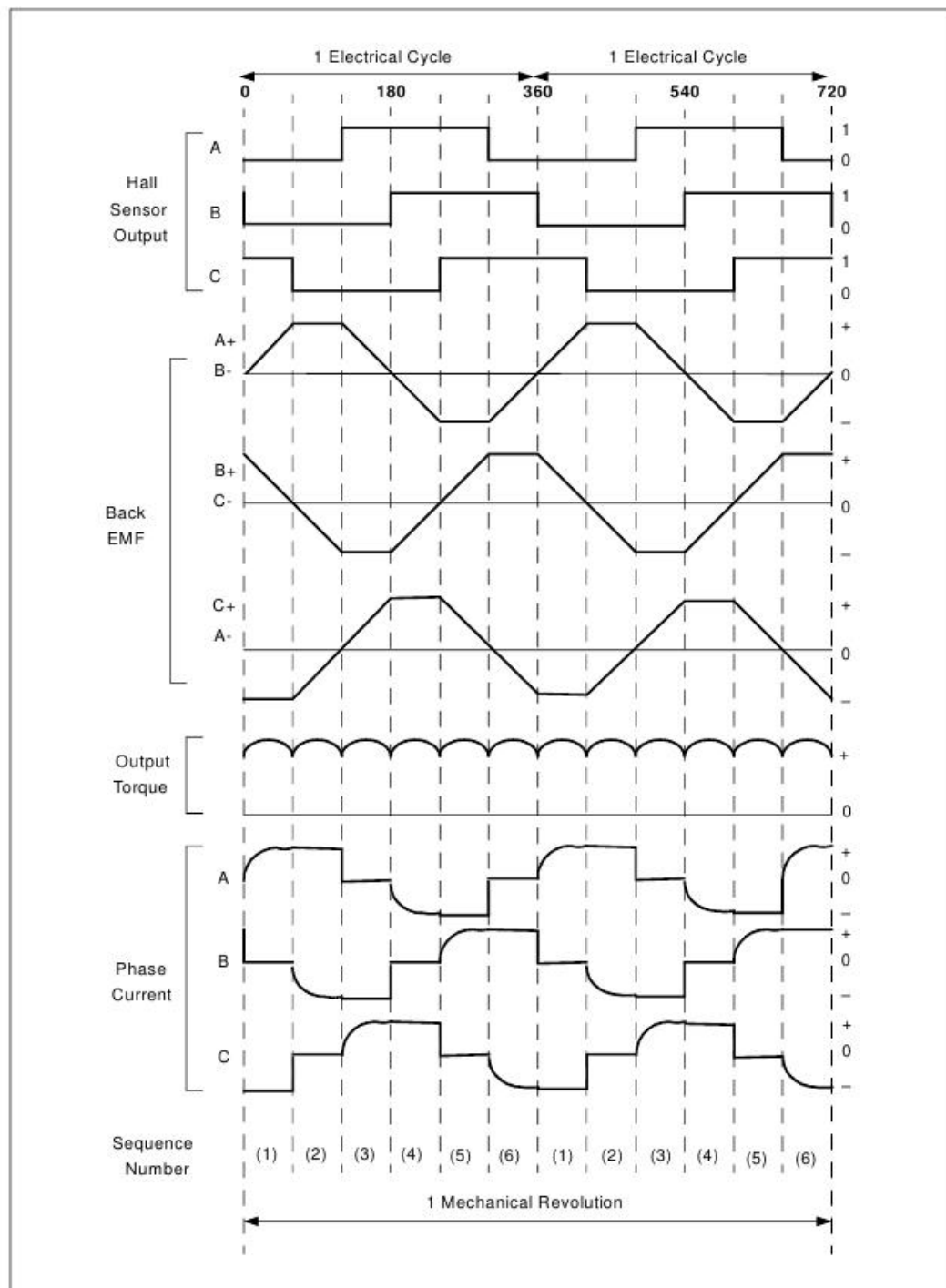


Figure 1.1: Hall effect sensors signal, back emf, output torque and phase current (Yedamale, 2003)

between each lap. The total energy consumption of the vehicle after driving for 4 laps will be collected and the mileage will be calculated. Every team will have 3 attempts for mileage improvement.

1.2 Problem Statement

PMBLDC motor is better compare to brushed DC motor because brushless motor increases the efficiency by dropping the friction between the brush and the comutator which happens in brushed DC motor. However, the inefficient PWM in controlling the speed of the motor and the torque ripple cause by the phase current limits the efficiency of a PMBLDC motor.

There are three types of torque produced by a permanent magnet electric motor which are:

- cogging torque
- reluctance torque
- mutual torque

The cogging torque is produced by the interaction between the permanent magnet at the rotor and the stator slots. Cogging torque is an undesirable torque generated by the electric motor which dominates at low speed and results in speed ripple. Cogging torque can only be minimize by means of hardware tuning which includes altering the number of poles, teeth at the stator or editing the controller setting which changes the drive current waveform.

The reluctance torque is generated by the difference in position of the rotor and the phase induction at the rotor. The ripple produced by the reluctance torque could be negligible with a good number of poles and slots of the windings at the stator.

The third type of torque produced by PMBLDC motor is the mutual torque which is caused by the non-sinusoidal signal reaching the stator windings or the magnet at the rotor. Since the torque is generated by the current, ripple reduction for mutual torque could be achieved by fine-tuning the current signal.

The torque ripple occurs in PMBLDC is mainly contributed by the different rise and decay time of the phase current as shown in figure 1.1. The cogging torque does contribute to torque ripple in low speed but it's negligible at high speed. Torque ripple contributed by reluctance torque could also be ignored since the increasing number of poles and stator slot minimize the ripple. Mutual torque would be the major contributor to torque ripple due to the direct dependency on the current.

Based on figure 1.2 (a), the rate of decay of i_a is faster than the rate of increase of i_b . Therefore, at certain point where i_a reaches 0 but i_b still rising, there will be a surge in current at phase C, i_c . As the result, there will be a sudden drop in torque output. The same case happens as shown in figure 1.2 (c) where i_a drops slower than i_b causing an sudden drop in i_c and sudden increase in torque output. The same circumstances apply for i_a-i_c and i_b-i_c hence creating a ripple torque output.

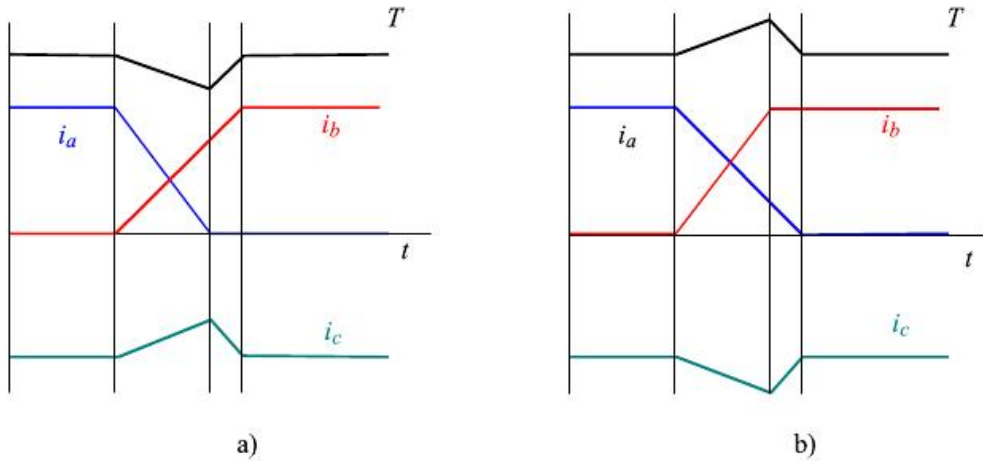


Figure 1.2: The phase current and torque during an alternating comutation event (Salah et al., 2011)

Apart from torque ripple in PMBLDC that reduce the efficiency of the electric motor and cut down the mileage of the electric vehicle, poor driving strategy will contribute to poor mileage. The Sepang North Track is a racing track that contains 3 uphill section and 3 uphill section and an approximately 800m long straight for the starting and ending line. This track is especially challenging for electric vehicle because the factor of torque generated by the electric motor, cruise speed when uphill and downhill, rolling resistance and drag factor need to be taken into consideration for minimum energy consumption.

1.3 Objectives

The objectives for this project are:

1. To identify the output signal of the controller circuit and the hall effect sensor of the PMBLDC and develop a set of instrument for measuring the mileage of the electric vehicle.
2. To study the track profile of Sepang North Track and create a simulation program for simulating the vehicle dynamics at the Sepang North Track.
3. To compose a set of strategy to increase the mileage of the electric vehicle running on the Sepang North Track based using the simulation program.

1.4 Scope of Research

In this project, the proprietary controller and PMBLDC motor signal output port will be identified. After that, by utilizing the signal output of the hall effect sensor and the controller speed output signal port, a set of instrument will be build for measuring the speed, input current and input voltage. The power input will then be calculated based on the voltage and current input.

Next up, the behaviour of the electric vehicle on the Sepang North Track will be simulated with taking the drag force, rolling resistance and track gradient into consid-

eration. With the frontal area, coefficient of drag, coefficient of rolling resistance and the mass of the vehicle as manipulating variables, a set of strategies could be created for electric vehicle at different mass, tyre pressure at the same track with using the same electric motor as drive train.

1.5 Research Approach

For tapping the signal from the PMBLDC motor's hall effect sensors as well as the analog/digital output from the controller circuit board for the speed signal, multimeter will be used. For building the measurement tools for measuring and logging the input voltage, input current and the speed of the vehicle, Arduino boards will be used in conjunction with the self-made transducing circuit.

For simulating the vehicle's behaviour on track, self-made codes using C++ language will be used for iteration. Data for each set of simulation and strategies will be saved and the graph will be plot for analysing the effectiveness of the strategy.

1.6 Summary

In this chapter, the background of PMBLDC motor and the electric vehicle for participating in Shell Eco-Marathon has been introduced. Furthermore, the trapezoidal shape winding voltage for PMBLDC has been described and the use of hall effect sensor for detecting the position of the rotor is explained.

The types of torque produced by PMBLDC motor is listed and the mutual torque has been identified as one of the problem contributor to the torque ripple for PMBLDC motor. The other problem raised up in this chapter is the poor racing strategy which cost us some mileage reduction during the Shell Eco-Marathon race.

The objectives for this project is listed which includes identifying the signal output of the proprietary controller and PMBLDC and build a measurement system for measuring the vehicle performance. Composing a set of strategies is one of the objectives

listed.

Finally, the scope of the research has been limited to the study of the vehicle dynamics, electric motor and the Sepang North Track for building the simulation software which is a self-built software using C++ coding language. The measurement system will be built using the Arduino microcontroller which has the ability to measure, log and display the voltage, current and the velocity.

CHAPTER 2

LITERATURE REVIEW

2.1 Introduction

In this chapter, the research paper of different researchers around the world will be reviewed. The research on tuning the PWM controller signal, modification of phase current signal for minimizing the torque ripple as well as driving strategy for cars and trains will be reviewed.

2.2 Torque Ripple

Park, Sung Jun *et al.* (Park et al., 2000) found that the back EMF generated by each of the three windings are slightly different in shape and magnitude from each other. Since the back EMF for each winding is different, therefore different phase current should be apply to each of the three windings. By assuming the three stator windings are in Y-shape connection, the cogging torque and the reluctance torque component is negligible and the mutual torque is directly proportional to the phase current, phase current for each of the three stator windings should be seperately excited in phase with the back EMF to minimize the losses and maximizing the torque-per-ampere generation.

Kim, Tae-Sung *et al.* (Kim et al., 2001) shows that by using the rectangular shape phase current that changes to high at the flat part of the back-emf wave can minimize the torque ripple, but this method is too ideal to be used in practical condition. In this paper, another method which is the unipolar PWM is introduced but it has a slow dynamic response, making this method not feasible at reducing the torque for current control commutation. The proposed current control algorithm is to seperate the phase current that contains all harmonic components to each harmonical components and then transformed into stationary frame. Then, each stationary frame is added together and

the output is the current command. After this process, the rectangular wave will appear more rectangular and hence reducing the torque ripple.

Nam, Ki-Yong *et al.* (Nam et al., 2006) suggested reducing the torque ripple by varying the input voltage to the PMLBLDC. The idea of this paper is that by maintaining the current at a constant value, the torque ripple could be minimized. The method for reducing the torque ripple used in this paper is to supply varied input voltage during the freewheeling region.

Wael A. Salah *et al.* (Salah et al., 2011) proposed a method which apply a modified PWM signal to the PMLBLDC. The modified PWM signal used will delay the build up of current in the in-coming phase gradually at low speed region. At high speed region, it will speed up the build up of current which results in overcoming the tips and dips of current during phase current commutation which contributes to reduce in torque ripple.

Mohamed. A. Enany *et al.* (Enany et al., 2010) presented a method for improving the performance of BLDC with varying the switch-on and switch-off angle of the phase current. By advancing the switch-on and switch-off phase current, it enables current at each windings to reach to the maximum value earlier hence reducing the tips and dips of the current at the other winding which results in reducing torque ripple.

G. H. Jang and C. J. Lee (Jang and Lee, 2006) proposed a method to reduce the torque ripple through eliminating cogging torque by implementing a modified current wave form. The modified current wave form consists of main and auxiliary wave which the main wave is the conventional wave whereas the auxiliary wave generates a torque which has the same magnitude but opposite direction to the cogging torque.

Vanisri A. and Devarajan N. (A. and N., 2011) describe the design of a controller with minimize torque ripple which different than the conventional controller for PM-BLDC motor by filter components. The methodology of the method used in this research is passing through the signal through an inductor-capacitor filter which filters

out the high frequency waveform. The capacitor is selected in a way that it can charge and discharge effectively and the inductor is responsible for reduce the current pulsation hence reducing the torque ripple.

Leila Parsa and Lei Hao (Parsa and Hao, 2008) studied the effect of magnetization, winding distribution, skew angle and current angle on torque pulsation minimization. The switching instance has been calculated in a way that the reluctance torque is utilized in reducing the torque pulsation. It is also shown in the paper that by using the proper switching interval and applying suitable current waveform, the torque pulsation is reduced.

2.3 Driving Strategy

Michiel Koot *et al.* (Koot et al., 2005) showed the work of analysing the engine, battery and alternator of an Hybrid Electric Vehicle (HEV). After the value of the parameters of an HEV is discretized, Dynamic Programming (DP) and Quadratic Programming (QP) techniques are used for the control strategy of the HEV.

Phil Howlett *et al.* (Howlett et al., 1997) discussed the making of an optimal strategy for a solar powered vehicle on a level road for participation in the World Solar Challenge. The draft strategy pointed out in the paper is:

- Accelerate using maximum available power.
- Hold speed at a lower critical speed, V, until mid-morning.
- Follow solar power up to an upper critical speed, W.
- Hold speed W until mid-afternoon.
- Follow solar power back down to the lower critical speed, V.
- Hold speed V until late in the afternoon.
- Follow solar power.

- Apply full regenerative braking, if available, or coast.
- Apply full regenerative braking and mechanical braking.

The mathematical model for the vehicle is built from the power flow from the solar panel to the traction system, from the battery to the traction system, from the solar panel to the battery and from the traction system to the battery. Vehicle dynamics, for instance, the rolling resistance and drag force were also modelled. Finally, the control strategy is made based on the mathematical model.

The paper written by Yasuo Shimizu *et al.* (Shimizu et al., 1998) introduced 2 system which is the Supervision Support System as shown in figure 2.1 and the Cruising Simulation as shown in figure 2.2. The Supervision Support System is a system where a control centre vehicle is followed behind the solar vehicle and collect all the data from the solar vehicle, the data is logged and calculated and the instruction is sent via transmitter back to the solar vehicle and displayed on the panel meters

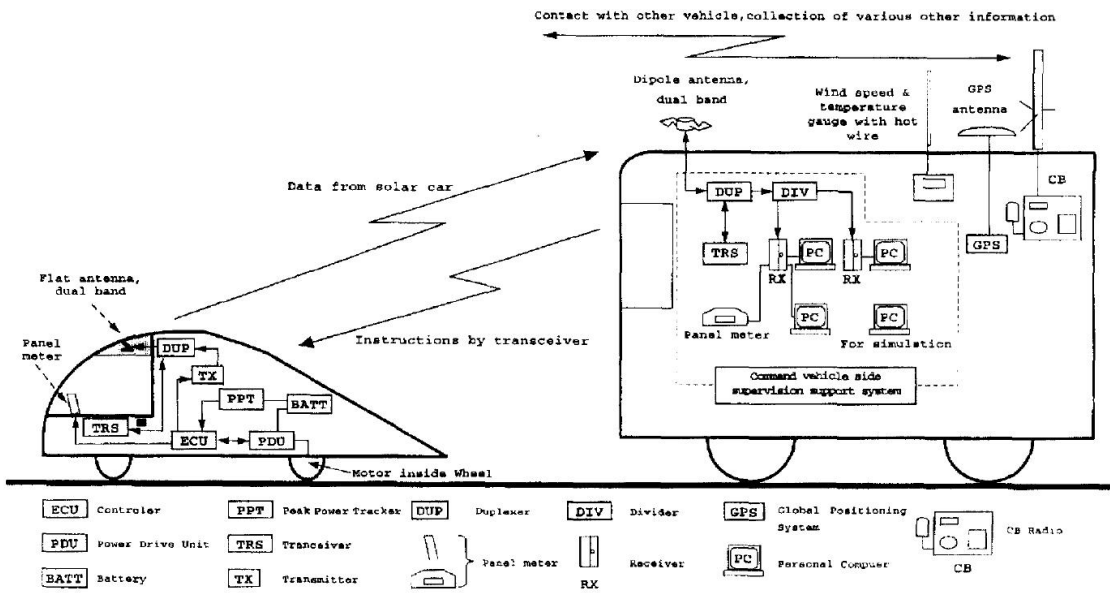


Figure 2.1: Supervision Support System hardware configuration schematic (Shimizu et al., 1998)

The Cruising Simulation on the other hand is a simulation process where the con-

dition component is set, for example, the environment condition settings, the vehicle specification settings and etc. Next, the result is calculated through calculation of every single condition, for instance, the reading of geographical data, the calculation of motor power and etc. By utilising the Supervision Support System and the Cruising Simulation, the on-road calculation could be done so that the power or speed control strategy can be set and implemented when the solar vehicle is running.

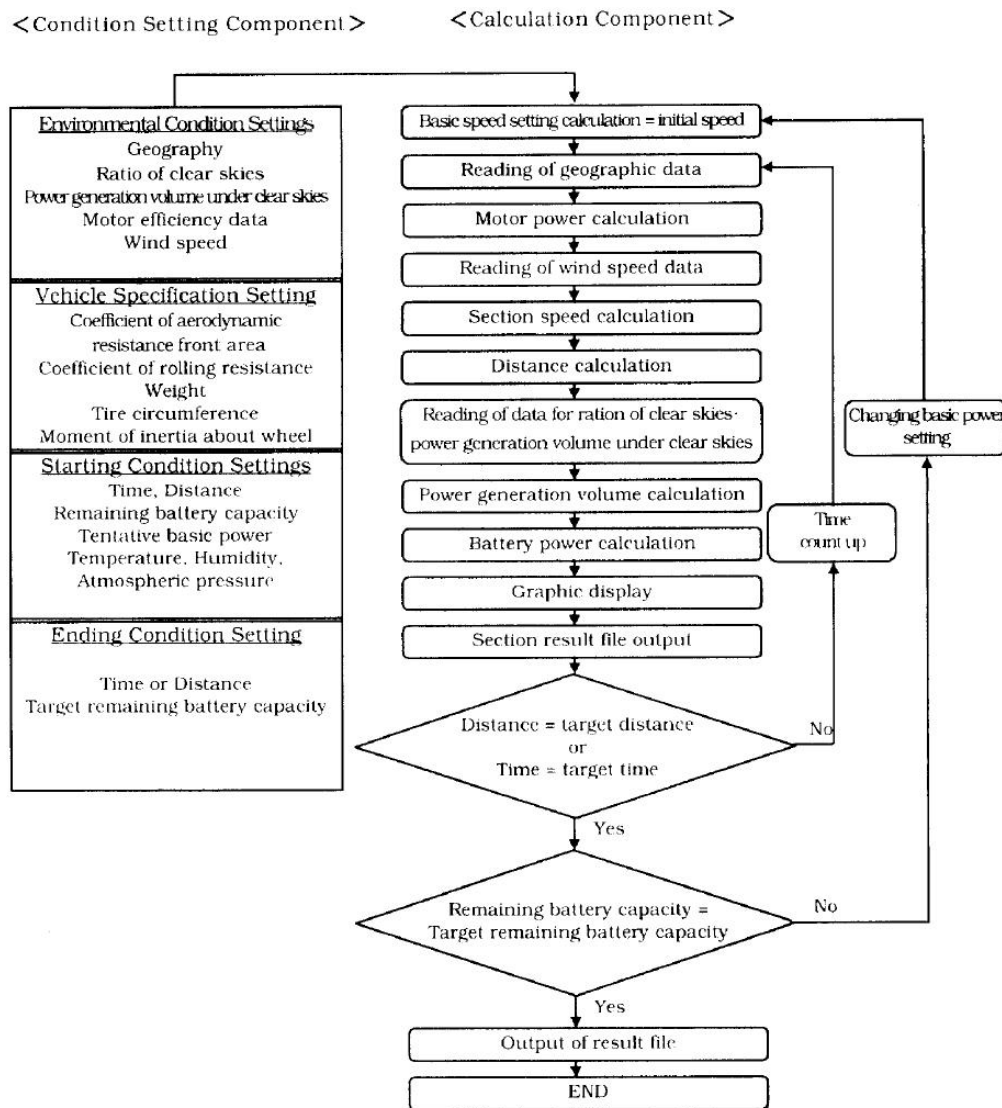


Figure 2.2: Flowchart of the Cruising Simulation (Shimizu et al., 1998)

Y.V. Bocharnikov *et al.* (Bocharnikov et al., 2007) researched on the optimal driving strategy for suburban railways. The strategy is constrained by two conditions which are energy saving and running fast so that it would not miss the schedule. There are 3 components for suburban railways which are the Motoring(M), Coasting(C) and Braking(B). By building mathematical model based on these 3 components and using fuzzy logic for optimization of energy function, a strategy with balance between the energy saving and running fast is achieved.

Peter Pudney and Phil Howlett Pudney and Howlett (1994) described building of strategies for a train journey which have speed limits at certain part of the journey. The method used in this paper is to build mathematical model for both the vehicle model and the journey model. Then, the speed profile was built and the optimal driving strategies were derived using mathematical models.

2.4 Summary

Various techniques for reducing the torque ripple have been reviewed in this chapter which includes using modified PWM signal, modifying the phase current and phase shifting the phase current. Apart from that, various strategies for solar car and train have been reviewed.

CHAPTER 3

METHODOLOGY

3.1 Introduction

In this chapter, the procedure for tapping the signal from the proprietary controller and PMBLDC motor and then building a performance measurement system based on the identified signal will be listed. Furthermore, the process of developing the mathematical model and the simulation of electric vehicle on Sepang North Track will be described so that the optimal mileage strategy could be identified.

3.2 Signal Identification

The drive train of the electric vehicle that will be used for participation in Shell Eco-Marathon consists of a single hub motor with no transmission. The hub motor is a PMBLDC motor, hence a controller is needed for controlling the speed as well as running the hub motor. The controller has two parts which is the controller circuit that is responsible for signal handling and a power unit which receives the signal from the signal handling unit and create the phase current for running the PMBLDC.

The signal unit of the controller takes input signal from the throttle, the key and also the hall effect sensors signal from the PMBLDC motor before it can do the calculation and output the signal to the power unit. Apart from that, the signal unit of the controller powers the speedometer and delivers the signal (for example: speed, battery voltage, vehicle mileage covered and the state of charge (SOC) of the battery) for displaying at the speedometer.

Since the speedometer acts solely as a display unit, it does not have signal outputs or data logging capability. Logging the data manually by reading and recording the speed,

voltage and SOC when the vehicle is running is appropriate because the electric vehicle is a single seater vehicle and it's impossible for the driver to drive and record the data simultaneously.

Therefore, the signals need to be tapped from the signal unit of the controller in order to build a system that is able to measure, display and log the data needed. Tapping all the signals is redundant because some reading is primary (for example the voltage) whereas some readings are derived from the primary signal (for instance, the SOC of the battery is based on the voltage). Hence, identification of the primary signals should be adequate.

There are a few signals that need to be tapped from the controller and the PMBLDC motor such as:

- Speed from the controller
- Voltage from the controller
- Hall effect sensors signal from the PMBLDC motor

Before the signal can be tapped and identified, the nature of the signal should be known. The voltage signal is an analog signal which is delivered directly from the battery through the controller. On the other hand, the speed signal should be an analog signal as well since the controller takes the signal of hall effect sensors, calculate the interval between each state change and multiply with the number of poles and the wheel diameter and get the speed of the vehicle as shown in equation 3.1, where V is the wheel speed, D is the wheel diameter, N is the number of poles of the PMBLDC motor and t is the interval between changing state of the hall effect sensor.

$$V = \frac{\pi D}{2Nt} \quad (3.1)$$

Figure 3.1 shows the hall effect signals which is a square wave. The hall effect sensor is a sensor where the output voltage from the sensor will change from minimum to maximum or vice versa depending on the circuit configuration. Since the sensor circuit is set in a way that it amplifies the signal and output high/low when the magnetic field of the rotor is detected as shown in figure 3.2, the signal output of the hall effect sensors is a square wave.

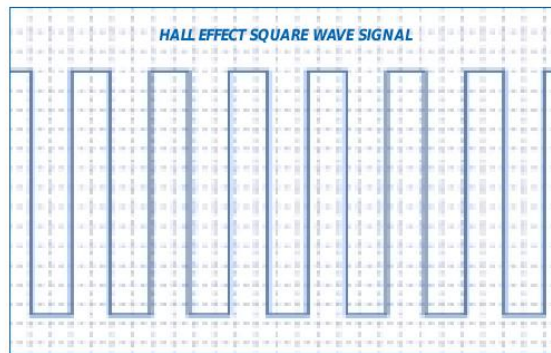


Figure 3.1: Hall effect sensor square wave signal (Point, 1999)

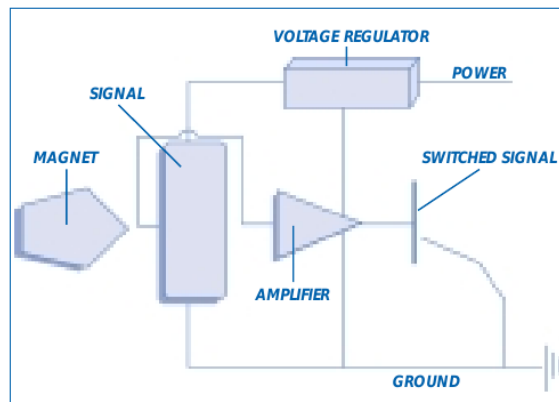


Figure 3.2: Circuit of hall effect sensor (Point, 1999)

There are 16 ports for signal and power from the controller to the speedometer as shown in figure 3.3. The method for detecting the signal is trial and error and elimination. The ground port is found using the digital multimeter where the two probes of the digital multimeter is plug in to any 2 ports. The port where it is constantly lower voltage than the other 15 ports is the ground port.

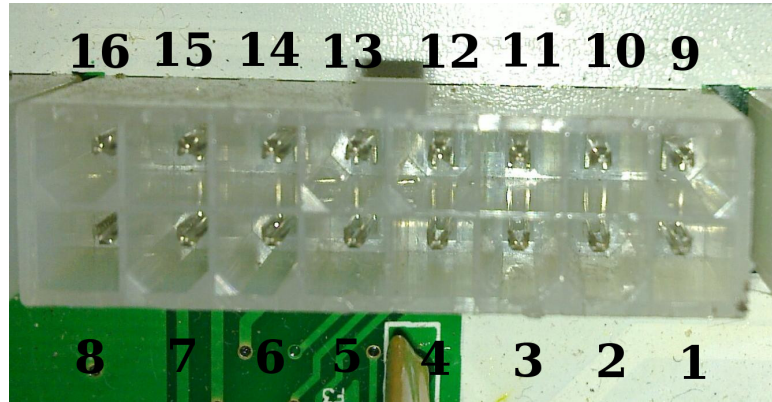


Figure 3.3: 16 pins controller circuit output

After the ground port is found, the procedure above is repeated by testing the 15 ports by taking the ground port as reference. The voltage reading for those 15 ports is measured and recorded when the system is idle and when the motor is running. The ports for the following signal should be found:

- Speed where the reading changes when the motor is rotating and static
- Battery voltage which it is at 50+V when the motor is idle and drops 2V when the motor is running
- A constant voltage 12V for powering the speedometer

The hall effect sensor terminal is a 8 ports input/output as shown in figure 3.4. Again, the method for detecting the signal is trial and error with step by step elimination that is similar to the method used for identifying the speed signal at the controller circuit. The hall effect sensor circuit has the same circuit that is shown in figure 3.2 except that it has 3 sensors signal output instead of 1 output.

The hall effect sensor tapping is started with the identification of the voltage input to the hall effect sensors circuit. The voltage input to the circuit is 12V, hence, using the same method as speed signal detection, the digital multimeter's probe is plug into the any 2 ports of the 8 I/O ports within the terminal and detect the port with 12V reading.

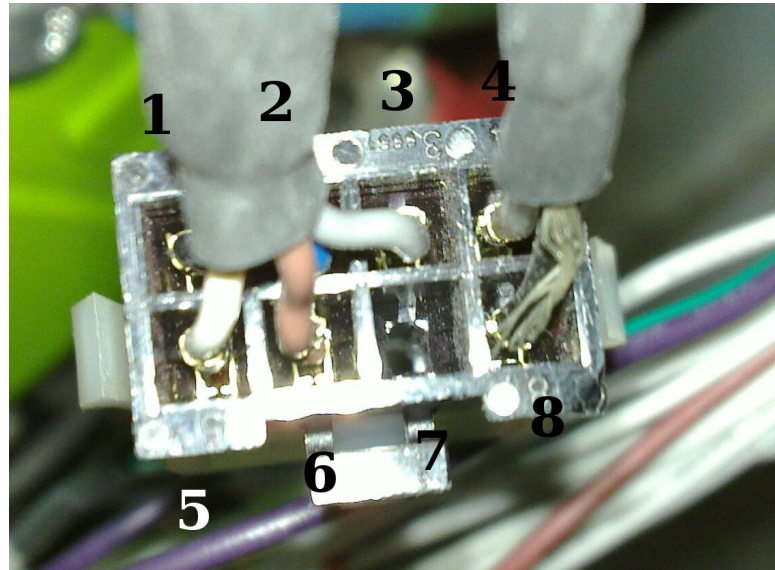


Figure 3.4: 8 pins hall effect sensor I/O

After the voltage input ports is identified, the 3 hall effect sensors output signal is tapped by again plugging in the ground probe to the ground input port and the other positive probe to any 1 of the 6 remaining ports. The wheel is rotated manually over a revolution and the ports that produce ups and downs voltage signal would be the hall effect sensors output port.

After the hall effect sensors output port has been identified, the probes of the multimeter is plugged into the first hall effect sensor output port and the ground port. The wheel is rotated by hand over a precise 1 revolution and the number of square wave over a wheel revolution is measured and the signal output at each 10° is measured and recorded. The same procedures apply to the other 2 hall effect sensors output ports. A graph of hall effect sensors signals versus the angle is then plot.

3.3 Measurement System

After the primary signal (speed and voltage) is identified, a measurement that has the ability to measure, display and log the parameters need to be built. The purpose of building the measurement system is to

- Measure and log the power consumption of the electric vehicle so that the mileage of the vehicle can be known.
- Measure and log the power consumtion at each vehicle on-road speed.
- Building a speed and power consumption display for the electric vehicle.

For measuring the power input, based on equation 3.2, the input voltage and input current need to be measured. Apart from measuring the power input to the electric vehicle, the data output from the measurement system can also be used to calculate the instantaneous deceleration of the vehicle when it's cruising, when it's braking with regenerative braking and when it's braking with regenerative and mechanical braking.

$$P_{input} = V_{input} I_{input} \quad (3.2)$$

The measurement system uses a circuit with microcontroller, crystal and I/O pins, which is the Arduino Mega 2560 board for processing the signal from the controller circuit, calculate the real value based on the signal, log the data into a SD card through the ITDB02 shield and display the speed and power consumption value through the ITDB02-3.2(WC) LCD screen.

Since the microcontroller board can only accept I/O less than 5V and more than 0V but the battery voltage is in the range of 48V - 60V and the speed signal from the controller is negative voltage, hence an intermediate circuit has to be built so that the signal can be read by the microcontroller.

For the voltage measurement circuit, a voltage divider is built for measuring the voltage of the battery. The voltage divider is a 2 resistor circuit that has same or different value of resistance for each of the resistor as shown in figure 3.5 The voltage output, V_{out} can be calculated using equation 3.3 where $R1$ is the resistance for the first resistor, $R2$ is the resistance of the second resistor and V_{in} is the voltage that need to be measured.

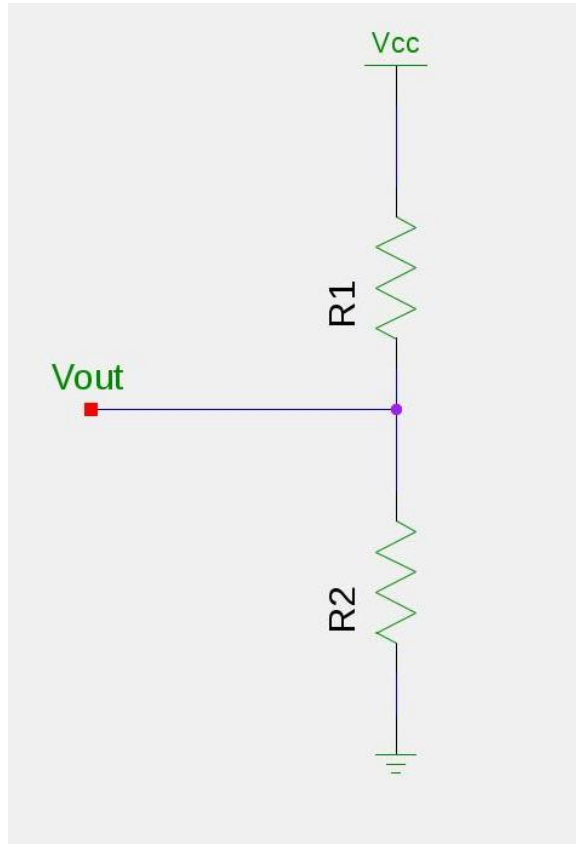


Figure 3.5: Voltage Divider

$$V_{out} = \frac{V_{in}R2}{R1 + R2} \quad (3.3)$$

For measuring the speed, the same method which is the voltage divider is used with a little modification which replaces the V_{in} to +5V and the ground to V_{in} as shown in figure 3.6 The V_{out} for the modified voltage divider circuit could be calculated using equation 3.4

$$V_{out} = \frac{(5 - V_{in})(R2)}{R1 + R2} + V_{in} \quad (3.4)$$

The resistance is selected based on the value of the negative voltage. For example, if the negative voltage is -5V, 1kΩ resistor can be selected for both $R1$ and $R2$ which yields:

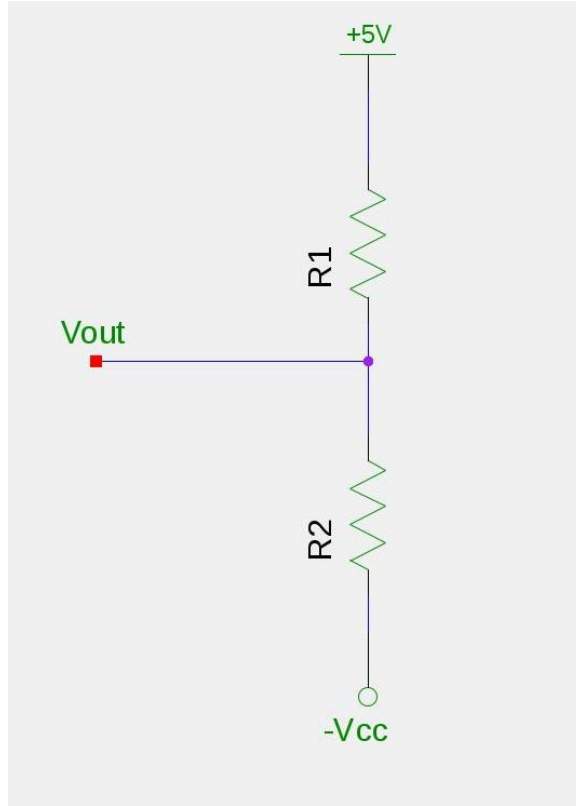


Figure 3.6: Voltage Divider for negative voltage

$$V_{out} = \frac{(5+5)(1000)}{1000+1000} - 5$$

$$V_{out} = 0V$$

If the V_{in} is 0V, V_{out} will be:

$$V_{out} = \frac{(5+0)(1000)}{1000+1000} - 0$$

$$V_{out} = 2.5V$$

Therefore, using a voltage divider, a negative voltage can be converted to positive voltage with minimum half of the original resolution.

The third parameter that need to be included in the measurement system is the input current. The input current is needed for calculating the input power to the electric vehicle and thus the overall vehicle mileage can be calculated. Since the rules of Shell Eco-Marathon restricted the nominal current input to the electric vehicle to be 60A and the peak current must be less than 150A, therefore a 200A current sensor is used.

The current sensor used in detecting the input current is the ALLEGRO MICROSYS-TEMS ACS758ECB-200B-PFF-T which is a 200A current sensor with 5 terminals and analog voltage output signal. In order for the microcontroller to measure the current, a current measuring circuit with the current sensor is built.

After the prototype circuit of the current measuring circuit, the voltage measurement circuit and the speed voltage divider circuit is built, the 3 circuits is integrated into a single circuit and the microcontroller is program in a way that it can read, log and display the speed of the vehicle, the instantaneous current and voltage and the mileage covered every 100ms interval.

3.4 Vehicle Simulation

The purpose of simulating the vehicle behaviour on the Sepang North Track is to get a list of parameter so that the suitable battery could be selected as well as optimum power saving could be achieved. By simulating the vehicle running on the track, the instantaneous acceleration, speed, required torque, power output, current, total energy consumption and total time could be acquired.

Since there is no free software in the market currently that has the ability to simulate an electric vehicle and heavily customized for simulating the electric vehicle that would be used in Shell Eco-Marathon, a simulation software is written.

The first step of building a simulation software is to build mathematical models for various components for vehicle dynamics. The mathematical model for the track and the PMLBLDC motor need to be built so that the slope of the track and the power generation and consumption of the electric motor can be known.

3.4.1 Track

Figure 3.7 shows the gradient of the track. By observing the graph, it can be seen that the maximum gradient is 5% and the minimum gradient is -6%. The gradient of the

track can be discretized easily since the gradient is of integer value, meaning that it doesn't have 5.5% gradient. From figure 3.7 it also can be observed that the gradient has a minimum length of 25m and the length of each gradient is of $n \times 25m$ where n is any integer value, hence, a step of maximum 25m can be used to discretized the track gradient.

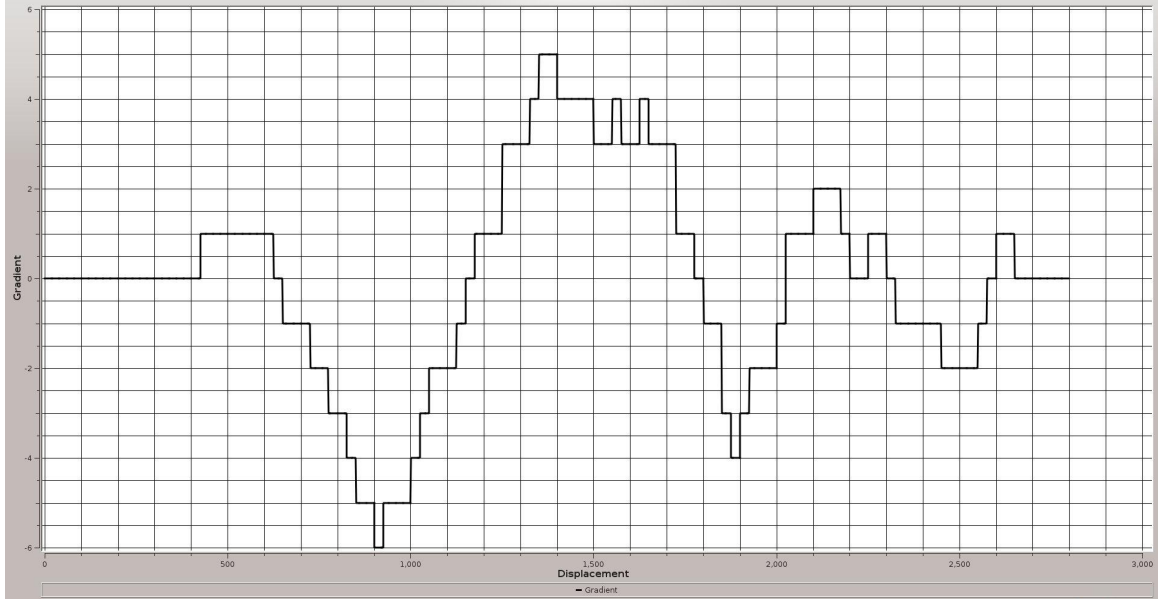


Figure 3.7: Track gradient of Sepang North Track

3.4.2 Electric Motor

Figure 3.8 shows the torque and power output profile of the KLD D1064R electric motor. The reason the KLD D1064R is used in the simulation is because the proprietary PMBLDC used in the electric vehicle is manufactured by KLD and this motor is the most similar to the electric motor that is used in terms of features, dimension and physical appearance.

The torque curve can be discretized into the mathematical model shown in equation 3.5. Since the throttle is a torque type controller, therefore the torque generated by the electric motor can be calculated from the mathematical model for the torque of electric motor times the amount of throttle applied.

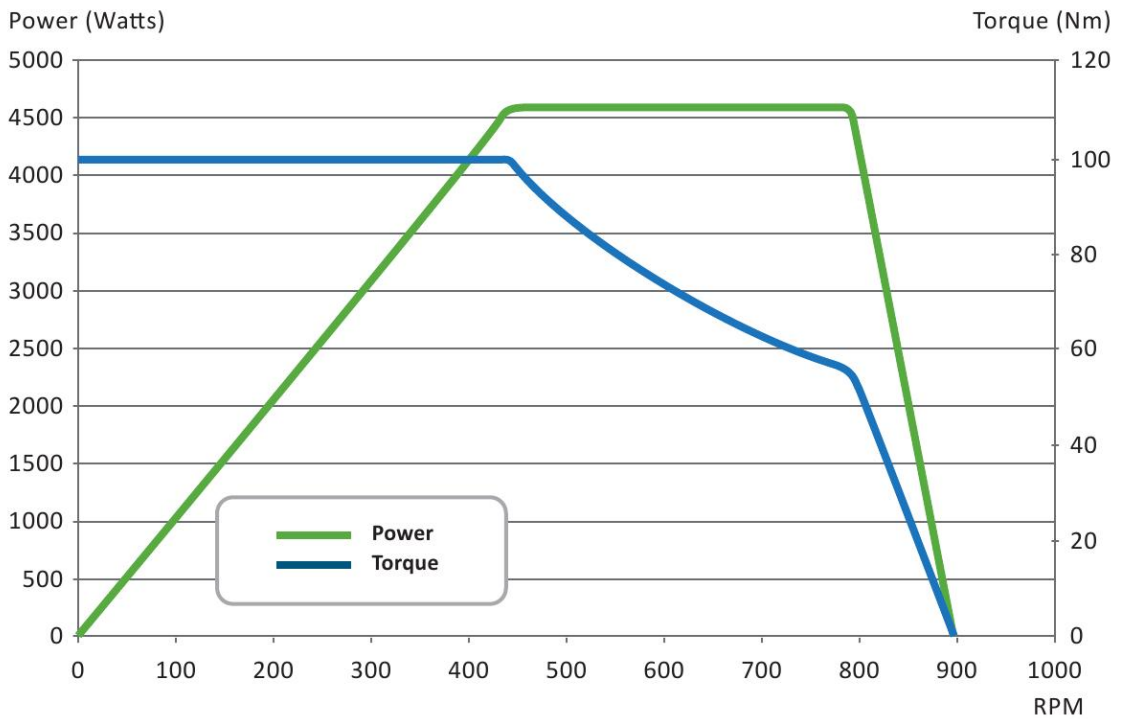


Figure 3.8: Torque and power output curve for KLD D1064R (Technologies, 2010)

$$T = \begin{cases} 100N.m, & \text{for } (0 - 440 \text{ RPM}) \\ [0.0003(RPM)^2 - 0.493(RPM) + 260]N.m, & \text{for } (441 - 800 \text{ RPM}) \\ [-0.56(RPM) + 504]N.m, & \text{for } (801 - 900 \text{ RPM}) \end{cases} \quad (3.5)$$

The power output curve of the electric motor shown in figure 3.8 is the product of torque and rotational speed, which is represented in equation 3.6 where τ is the torque and RPM is the motor rotational speed at revolution per minute.

$$P_{output} = \frac{(\tau)(2\pi)(RPM)}{60000} \quad (3.6)$$

3.4.3 Air Drag Force

The drag force by air drag exerted on a vehicle is directly proportional to the Coefficient of Drag (C_d), the frontal area of the vehicle, the density of the fluid, which in this context is the density of the air and also the square of the vehicle speed. By assuming the wind speed is 0 and no wind coming from any direction, the air drag force can be represented by the mathematical model shown in equation 3.7 where ρ is the density of the air, C_d is the coefficient of drag, A is the frontal area of the vehicle and v is the speed of the vehicle.

$$F_{drag} = \frac{1}{2}\rho C_d A v^2 \quad (3.7)$$

3.4.4 Rolling Resistance

The rolling resistance on the electric vehicle can be calculated using equation 3.8 where mg is the weight of the vehicle and C_{rr} is the coefficient of rolling resistance of the vehicle.

$$F_{roll} = mgC_{rr} \quad (3.8)$$

3.4.5 Slope

When the vehicle is driving along a track that has lots of slope, for instance, the Sepang North Track, the uphill slopes will contribute to the resistance to the vehicle. The uphill and downhill force can be model using the equation 3.9 where mg is the weight of the vehicle and θ is the angle of the slope in $^\circ$.

$$F_{slope} = mg \sin \theta \quad (3.9)$$

3.4.6 Vehicle Acceleration

The acceleration of the vehicle can be calculated using the Newton's Second Law of motion which is shown in equation 3.10. The parameter m is the mass of the vehicle whereas the parameter a is the acceleration of the vehicle.

$$F = ma \quad (3.10)$$

3.4.7 Combine Mathematical Model

After the mathematical model of the uphill/downhill, rolling resistance, air drag force and vehicle acceleration has been built, those mathematical equations are combined forming a combined mathematical model for simulation of vehicle dynamics. The combined mathematical model is shown in equation 3.11. $\sum F_{resistance}$ is the total resistance force exerted to the electric vehicle. By ignoring the ambient temperature, weather condition and opposing wind speed, the mathematical model generated in equation 3.11 can be used to simulate the dynamics of the electric vehicle.

$$\sum F_{resistance} = mg\sin\theta + mgC_{rr} + \frac{1}{2}\rho C_d A v^2 \quad (3.11)$$

The acceleration or the deceleration of the electric vehicle can be calculated using equation 3.12, where τ is the torque generated by the electric motor, R is the radius of the wheel attached to the hub motor, $\sum F_{resistance}$ is the total resistance force calculated using equation 3.11 and m is the total mass of the electric vehicle.

$$a = \frac{\left(\frac{\tau}{R} - \sum F_{resistance}\right)}{m} \quad (3.12)$$

3.5 Summary

The methodology for this project starts with the signal identification for the proprietary controller and PMBLDC motor. After the output signal for the speed and voltage has been identified, the voltage, current and speed measurement circuit has been built. The measurement circuit is able to measure, log the measurement result and display the parameters. Next, simulation program is built for simulating vehicle dynamics. With using the simulation program, a set of strategies can be composed.

CHAPTER 4

RESULT AND DISCUSSION

4.1 Introduction

In this chapter, the result of signal identification will be displayed and explained. Furthermore, the result of the measurement system which includes the schematic of the system will be shown. After that, the vehicle simulation program and the result of 1 lap of simulation around Sepang North Track will be displayed and discussed. Finally, several strategies planned using the simulation software will be shown follow by discussion on which strategy is better and comparison between the strategies.

4.2 Signal Identification

The result of signal tapping for the 16 pin controller circuit output is tabulated. Table shows the result of signal tapping with the ground probe on pinout 1 and voltage terminal for pin 2 to pin 15. From the table, all the reading is in negative voltage, hence indicating that the pinout 1 might be the battery voltage output.

The result of ground probe at pinout 2 is shown in table The battery positive voltage pinout is identified as pinout 1, the 12V power supply for the speedometer is identified as pinout 3 and pinout 2, 6 and 11 is identified as ground.

The result of placing the ground probe to pinout 2, running the motor and detect the voltage for 15 others pinout is shown in table It can be see that the battery voltage drops slightly as the motor spins up and pinout 4 give a negative voltage result. The voltage of other pin remains unchanged when the electric motor is rotating indicates that the pin 4 is the speed signal output port.

The result of tapping the hall effect sensor signals for 10°interval is shown in table The 3 hall effect sensors output is identified as pin ..., ... and ..., the positive 12V supply voltage for the hall effect sensor is pin ... and the ground is pin The pattern of the hall effect sensor is plot and shown in figure The total number of poles for the PMBLDC is identified as 28 poles judging from the hall effect sensors signal.

4.3 Measurement System

The measurement system that has the ability to measure the input voltage, input current and speed of the vehicle is built. Figure ... shows the schematic of the intermediate circuit for connecting the output signal from the controller circuit to the Arduino microcontroller.

The job of displaying the measured parameter and logging it into a SD card is done by the ITDB02 shield and the ITDB02-3.2WC LCD screen, the combination of the Arduino microcontroller, the shield and the LCD display is shown in figure ...

4.4 Vehicle Simulation

The vehicle dynamics simulation software is built. As explained in last chapter, the simulation software has the ability to simulate the vehicle behaviour when driving around the Sepang North Track. As shown in figure 4.1, the software is initialized before the simulation can be started. The software takes a few parameters for initialization of the vehicle model which includes the vehicle driving wheel diameter, the total mass of the electric vehicle including the mass of the driver, the frontal area of the electric vehicle, the coefficient of rolling resistance and the coefficient of drag. The parameters for initializing the vehicle model are shown in table 4.1.

The motor and track model is initialized at the second and third tab of the initialization dialog as shown in figure 4.2 and figure 4.3. At the last tab, the displacement interval for iteration is set which has a range from 1m to 25m, which is shown in figure 4.4.

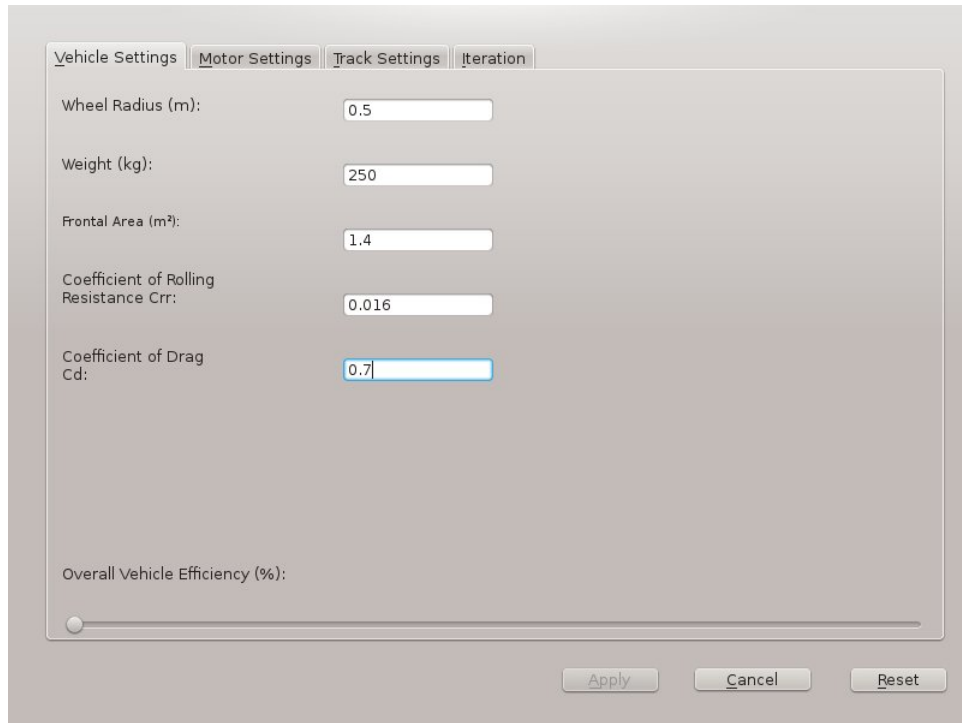


Figure 4.1: Vehicle parameter for initializing the vehicle model

Parameter	Value
Wheel Radius	0.5 m
Total Vehicle Mass	250 kg
Frontal Area	1.4 m ²
Crr	0.016
Cd	0.7

Table 4.1: Parameters for building the electric vehicle model

The simulation was run using "full throttle everywhere" strategy. The "full throttle everywhere" is the fundamental strategy for building the baseline data by applying full throttle over the entire circuit, which would give a maximum energy consumption result. The graph listed below is plot based on the simulation result:

- Speed and gradient versus displacement
- Power and gradient versus displacement
- Air drag versus displacement

The graph of vehicle speed and track gradient versus the displacement is shown in

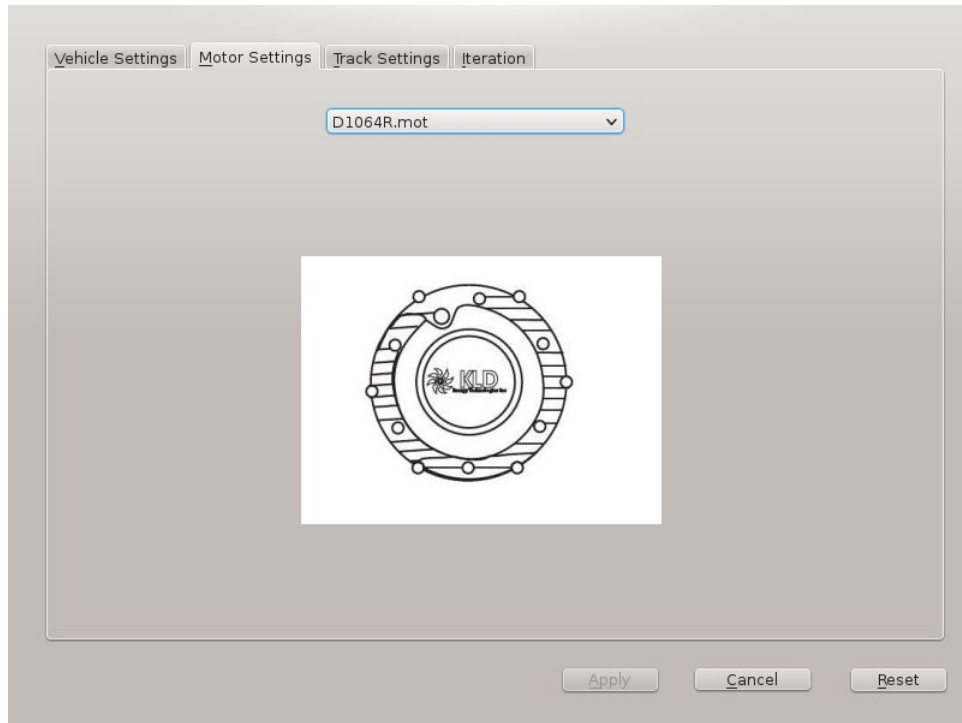


Figure 4.2: Choosing the motor model

figure 4.5. According to the graph, the maximum speed is 20.6m/s. The maximum speed is achieved at 1100m where the vehicle is driving downhill. The speed of the vehicle fluctuates between 20.6m/s and 12.6m/s from 1100m displacement onwards until end of the lap. The vehicle speed varies with the pattern of the gradient which it slows down when going up the hill because the torque generated is less than the total resistance torque exerted on the vehicle. The electric vehicle speeds up when going down the hill simply because the torque generated is excessive.

Figure 4.6 shows the power and gradient versus displacement. The power profile is the same as the speed profile as the torque generated by the electric motor is the same throughout the whole circuit which is constant 100N.m output. This is because the maximum torque output of the motor below 800RPM is 100N.m. The maximum power output of the electric vehicle is at around 1000m with a value of 4050W.

Figure 4.7 displays the graph of air drag versus displacement. Again, the air-drag profile is similar to the vehicle speed curve because the air-drag force is proportional to the square of the velocity of the vehicle. The maximum air drag occurs when the

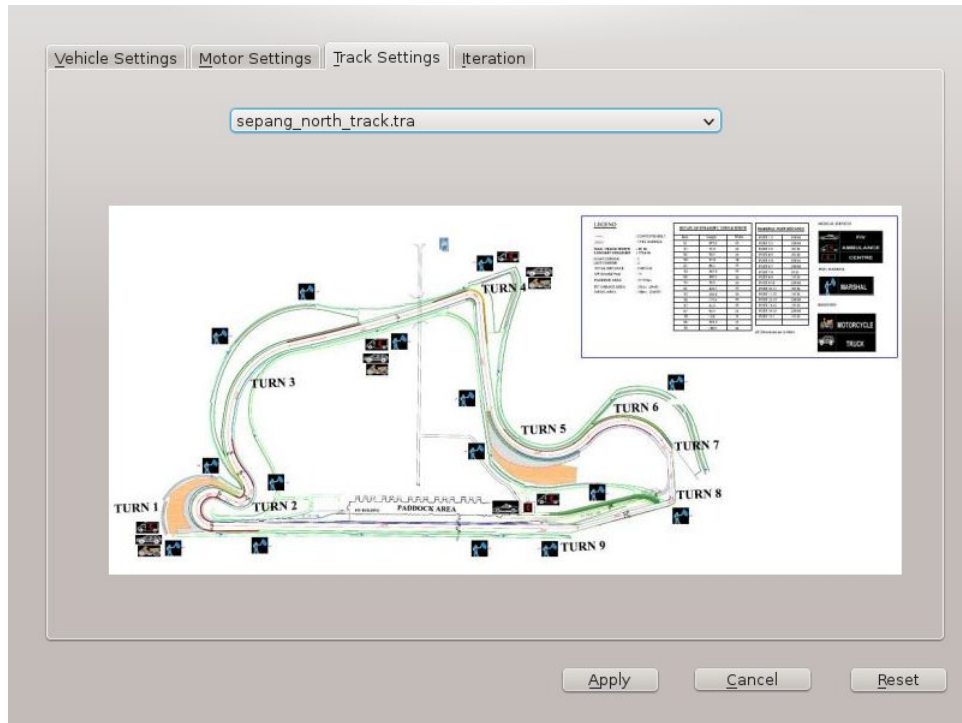


Figure 4.3: Choosing the track model

speed of the vehicle hits maximum with the magnitude of 120 N.m of torque needed for overcoming the air-drag.

Table 4.2 shows the main result for the "Full Throttle Everywhere". As shown in the table, the total energy consumption as simulated is 560003J and the lap time is 187 seconds. The total time for 4 laps will be 748 seconds, with 10 seconds of stops between each lap and some time wasted, the time for completion for 1 attempt will be 788 seconds which is 13 minutes and 8 seconds. The mileage calculated from the energy consumption is 18 km/kWh.

Result	Value
Total Energy Consumption	560003J
Total Time for 1 Lap	186.981s
Mileage	18 km/kWh

Table 4.2: Main result for "Full Throttle Everywhere"

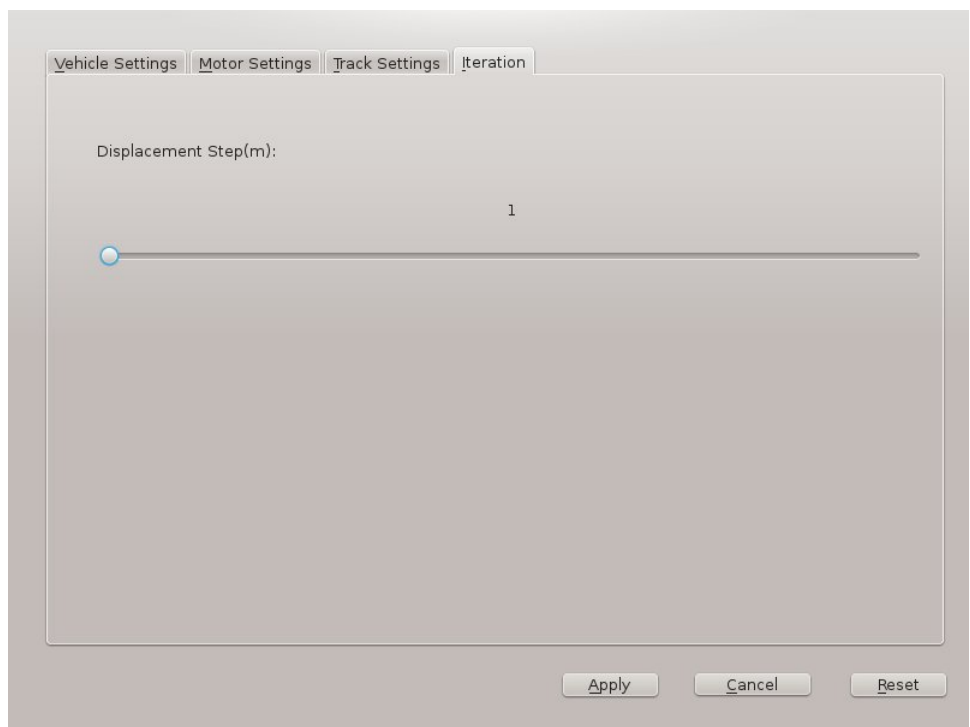


Figure 4.4: Setting the displacement interval for iteration

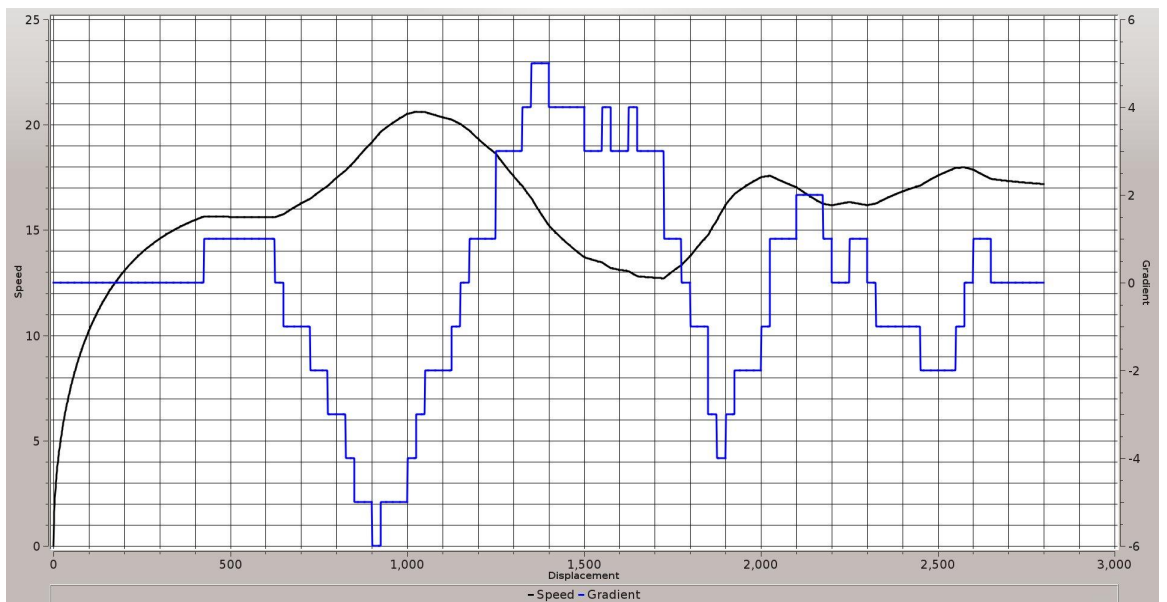


Figure 4.5: Graph of speed and gradient versus displacement for "full throttle everywhere"

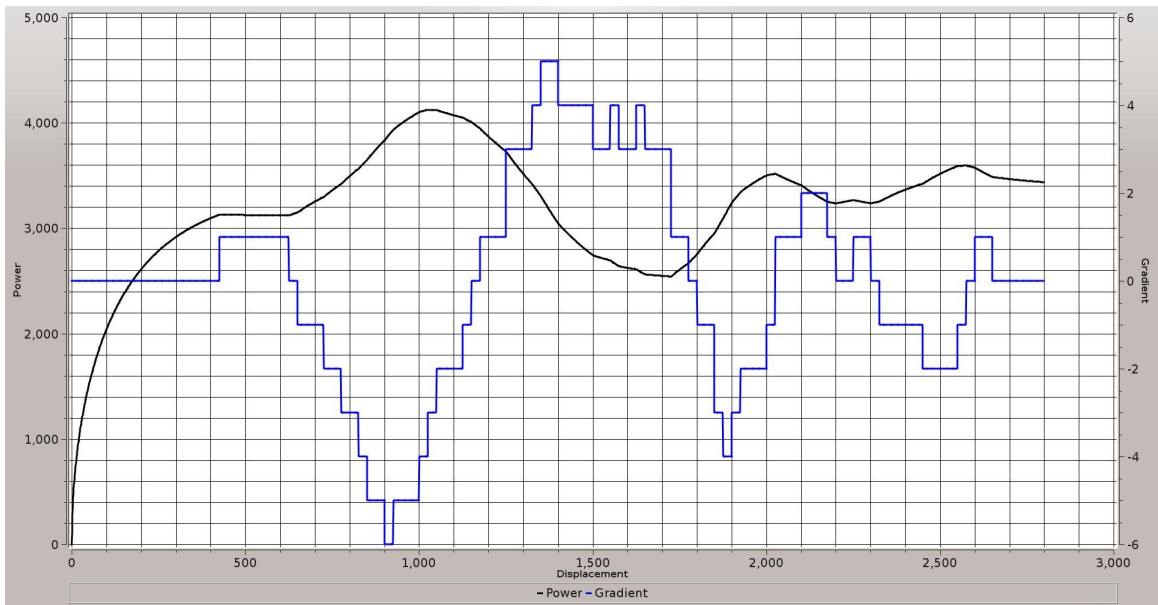


Figure 4.6: Graph of power and gradient versus displacement for "full throttle everywhere"

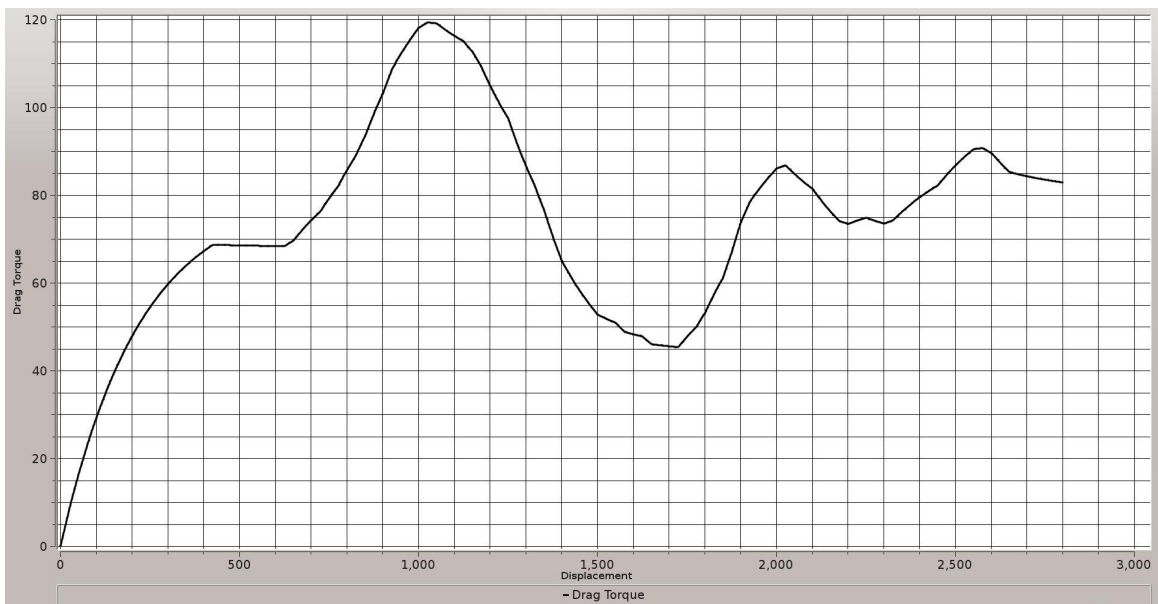


Figure 4.7: Graph of air drag versus displacement for "full throttle everywhere"

4.5 Strategies

There are 3 strategies composed for improving the mileage of the electric vehicle on the Sepang North Track.

4.5.1 Preset Strategy 1

The "Full Throttle Everywhere" strategy listed at the previous section is not effective because the torque generated by the electric motor is excessive at most of the part of the circuit. Therefore, a better strategy is produced which is the "Preset Strategy 1". The "Preset Strategy 1" reduces the energy consumption of the electric vehicle by turning off the electric motor so that the electric vehicle cruise down the hill when the gradient is less than 0° . By using the simulation software, the result of "Preset Strategy 1" is shown at the following graphs.

Figure 4.8 shows the graph of speed and gradient versus displacement for "Preset Strategy 1". The speed profile of the electric vehicle shown in this graph is different with the speed curve in figure 4.5 since the vehicle is set to cruise when the gradient is negative. The maximum speed of the vehicle is less than the maximum speed for "Full Throttle Everywhere" strategy which has a value of 15.7m/s and happens at the end of starting straight. The speed of the vehicle drops gradually when going downhill because the gravitational force is insufficient for countering the rolling resistance and air drag. The vehicle pick up speed when the gradient of the track is less than 3° and started to slow down when the gradient is higher due to the inadequate torque generated by the electric motor.

Figure 4.9 shows the graph of power and gradient versus the displacement for "Preset Strategy 1". The power curve shows a huge rise at the beginning straight. The power output of the electric vehicle is 0 when cruising down and the power output surge again when the vehicle is driving on the flat road or up the hill. Since the speed of the vehicle is less than the speed of the vehicle in "Full Throttle Everywhere" strategy, the maximum output also drops from over 4kW for the previous strategy to around 3.1kW for

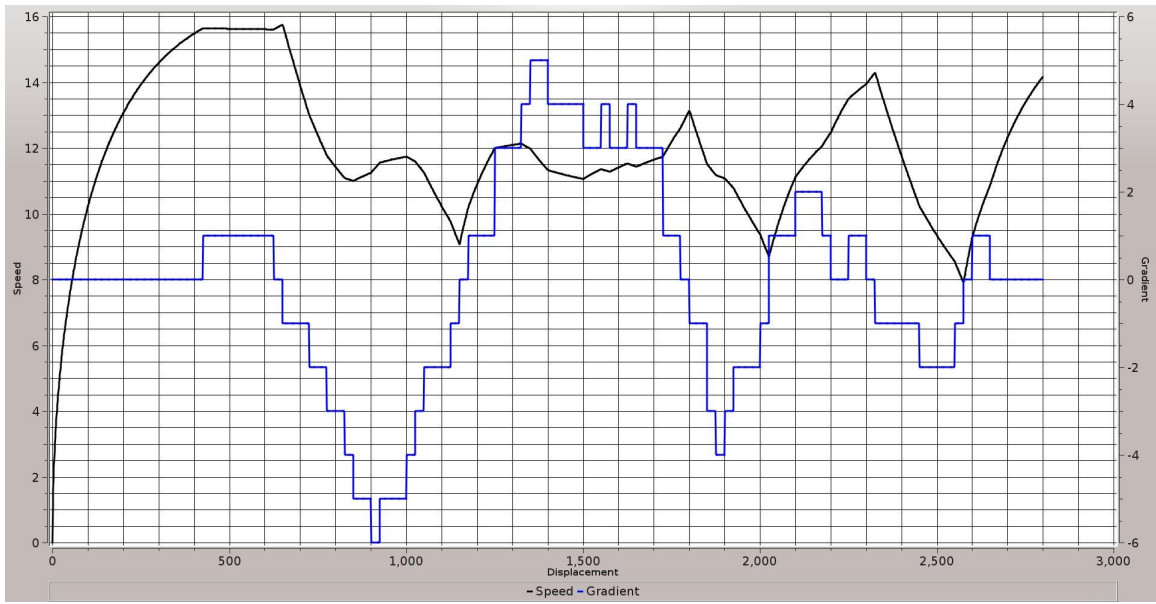


Figure 4.8: Graph of Speed and Gradient versus displacement for "Preset Strategy 1"

the current strategy.

Since the maximum vehicle speed is reduced by 23.8% , the maximum torque need to be supplied by the electric motor for counter air drag force reduces from 120 N.m to 69.5 N.m, which is a huge 42% improvement as shown in figure 4.10.

Table 4.3 shows the overall result simulated using "Preset Strategy 1". The total energy consumption is reduced to 365004J but the lap time is increased to 247 seconds. The time for 1 attempt is increases to 1026 seconds which is 17 minutes and 6 seconds which is within the time limit. The mileage using Preset Strategy 1 is improved to 27.6 km/KWh.

Result	Value
Total Energy Consumption	365004J
Total Time for 1 Lap	246.554s
Mileage	27.6 km/kWh

Table 4.3: Main result for "Preset Strategy 1"

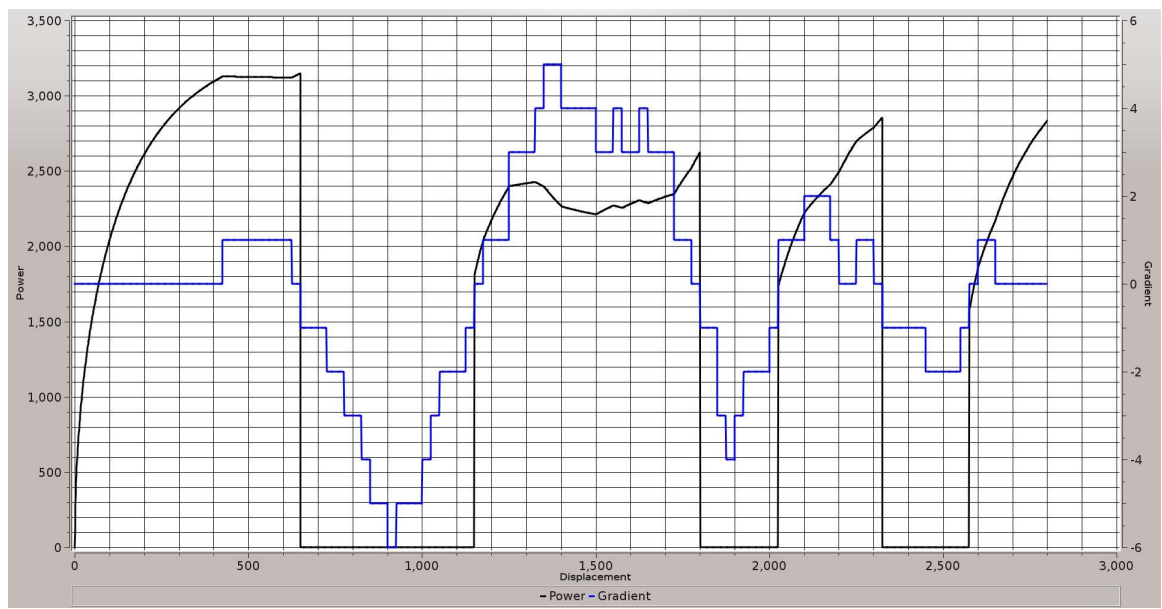


Figure 4.9: Graph of Power and Gradient versus displacement for "Preset Strategy 1"

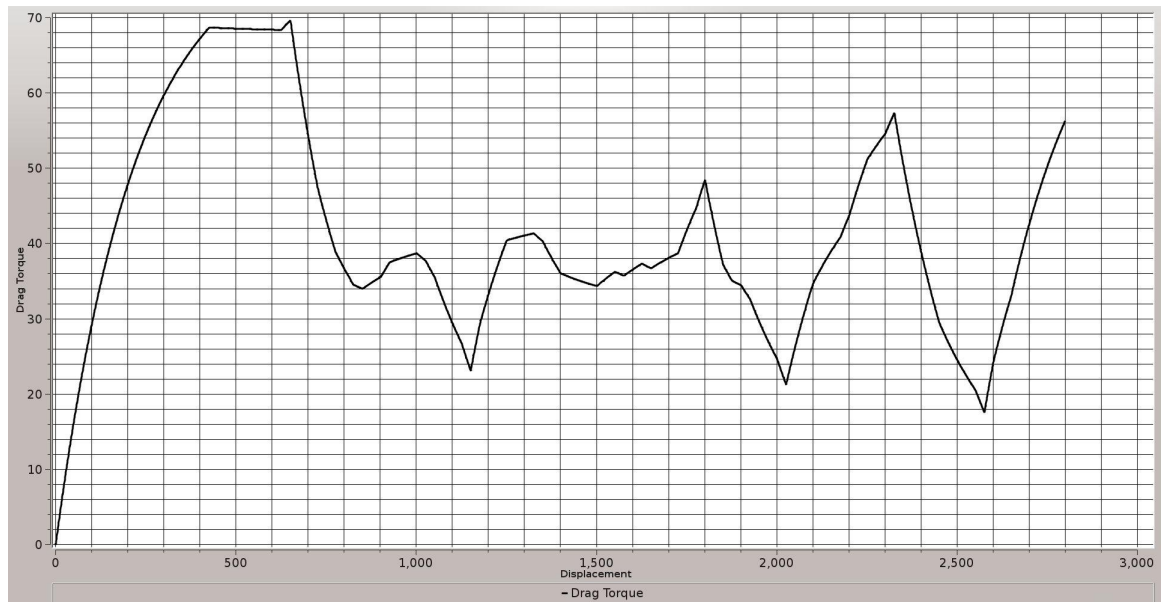


Figure 4.10: Graph of air drag versus displacement for "Preset Strategy 1"

4.5.2 Preset Strategy 2

Since the "Preset Strategy 1" waste a lot of energy by accelerating through the ending straight and the speed of the vehicle is still reducible for reducing the effect of air-drag, "Preset Strategy 2" is set so that the vehicle cruise to the end of a lap and the speed is controlled within 14m/s and the vehicle started to cruise at 2650m displacement onwards until the start/finish line.

Figure 4.11 shows the graph of speed and gradient versus displacement. The speed curve is similar to the speed curve for "Preset Strategy 1" except that the top speed of the electric vehicle is limited to 14m/s by the strategy. The curve after 2650 displacement is also dropping which is different than previous strategy.

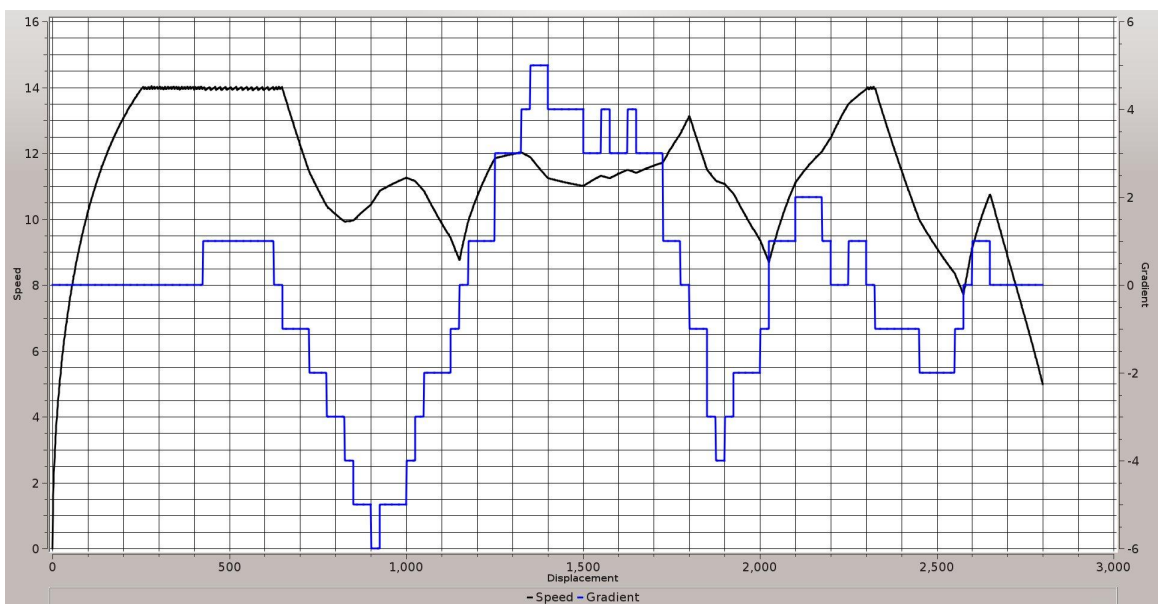


Figure 4.11: Graph of Speed and Gradient versus displacement for "Preset Strategy 2"

Figure 4.12 is the graph of power and gradient versus displacement. The power curve is similar to the power curve for the previous strategy with some minor difference which is the power output of the electric motor is 0 near the end of the circuit (after 2650m). In addition, lots of fluctuation is observed between 250m to 650m displacement. This is because the simulation set the throttle to 0 and 1 alternatively for maintaining the top speed at 14m/s which is similar to the principle of PWM. In real

life, switching between minimum and maximum throttle frequently will create lot's of current spike and hence waste more energy. Therefore, in actual race, the driver have to adjust the throttle so that the speed maintain at 14m/s.

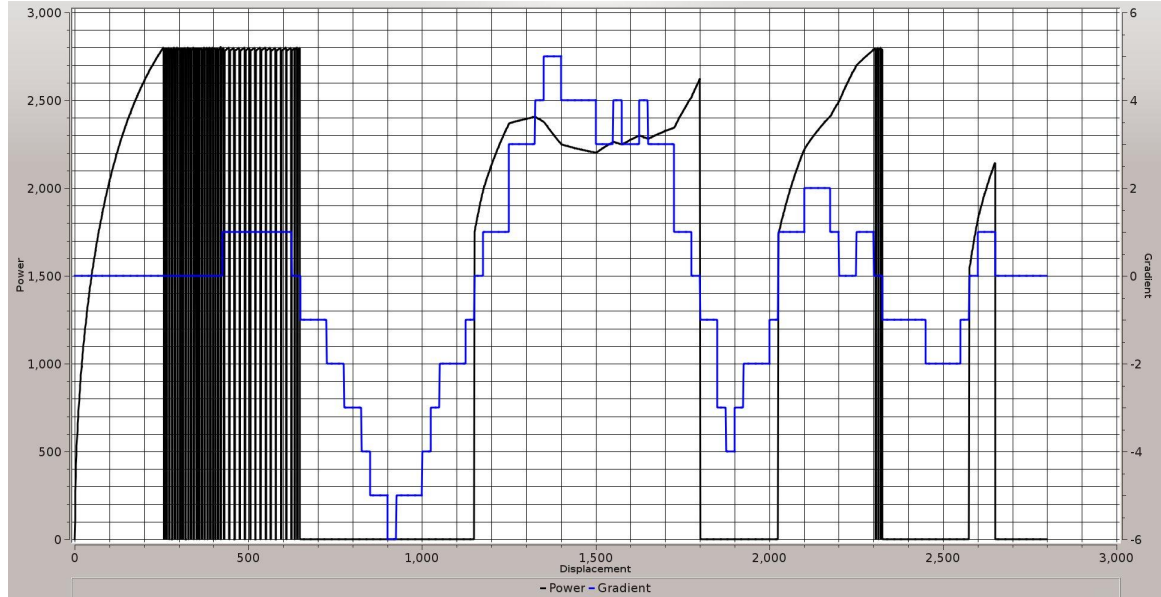


Figure 4.12: Graph of Power and Gradient versus displacement for "Preset Strategy 2"

Figure 4.13 shows the air drag versus the displacement for "Preset Strategy 2". As the maximum speed is limited to 14m/s, the maximum torque needed by the electric motor for countering the air drag drops to 52.5N.m which is another 24.5% improvement over the previous strategy.

Table 4.4 shows the main result for "Preset Strategy 2". As shown in the table the energy consumption is reduced to 318200J hence the mileage increases to 31.7km/kWh. Due to the top speed limitation, the average speed of the vehicle reduces. Therefore the lap time increases to 262 seconds yielding the total time for 1 attempt to be 1087 seconds which is 18 minutes 7 seconds.

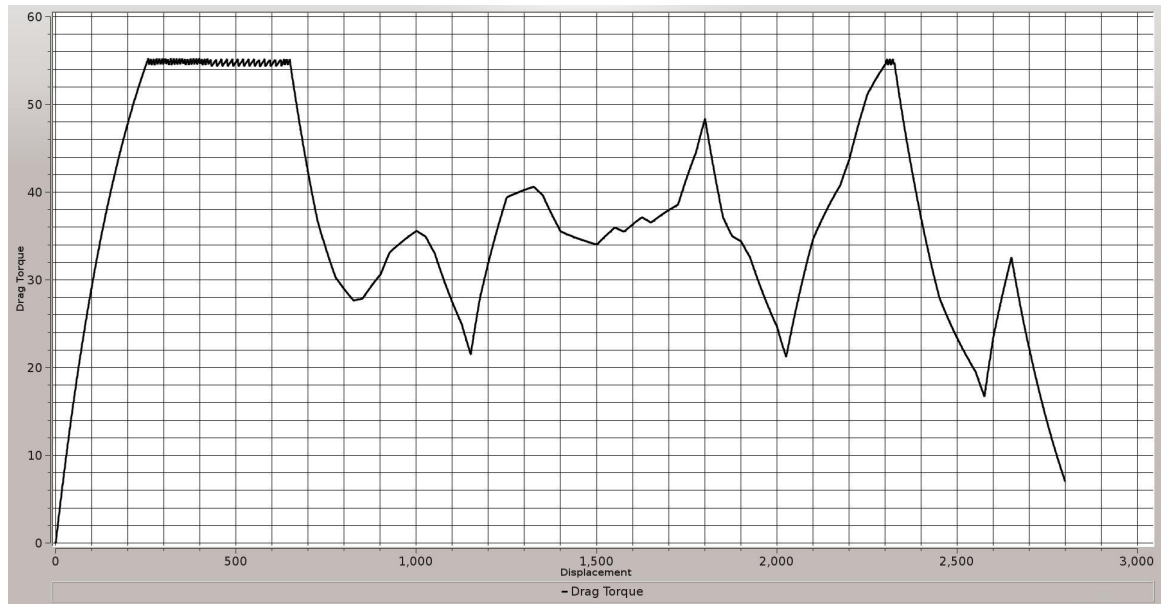


Figure 4.13: Graph of air drag versus displacement for "Preset Strategy 2"

Result	Value
Total Energy Consumption	318200J
Total Time for 1 Lap	261.699s
Mileage	31.7 km/kWh

Table 4.4: Main result for "Preset Strategy 2"

4.5.3 Preset Strategy 3

"Preset Strategy 2" reduces the energy consumption of the electric vehicle compared to "Preset Strategy 1" but there is still room of improvement because full throttle is applied when the vehicle is climbing so the generated torque at some section may exceed the required torque which will then accelerate the vehicle when driving uphill. Therefore, a new strategy is composed to tackle this problem which is the "Preset Strategy 3".

The "Preset Strategy 3" is a strategy which has the following characteristics:

- Gradual acceleration, limit the acceleration to 0.13m/s^2 .
- The speed is limited to 11m/s-12m/s at flat road before 2600m displacement.
- Vehicle accelerating softly to reach 8m/s after 2600m and cruising after 2750m displacement.
- Vehicle maintain at constant speed when driving up the slope.
- Vehicle cruising when driving down the slope.

Figure 4.14 shows the speed and gradient versus the displacement graph. From the graph, the maximum speed of the electric vehicle is reduced to 11.9m/s. The speed when the vehicle is driving up the hill is almost constant with low magnitude fluctuation due to the calculation of air drag using the previous velocity.

Figure 4.15 shows the power and gradient versus displacement graph. As shown in the graph, the power output of the electric vehicle matches the gradient of the track with some minor offset contributed by the acceleration of the vehicle and the air drag on the vehicle. The maximum power output power occurs at around 1350m displacement with a value of 1.75kW.

Figure 4.16 shows the graph of air drag versus displacement for "Preset Strategy 3". Again, the maximum torque required to overcome the air drag reduced from previ-

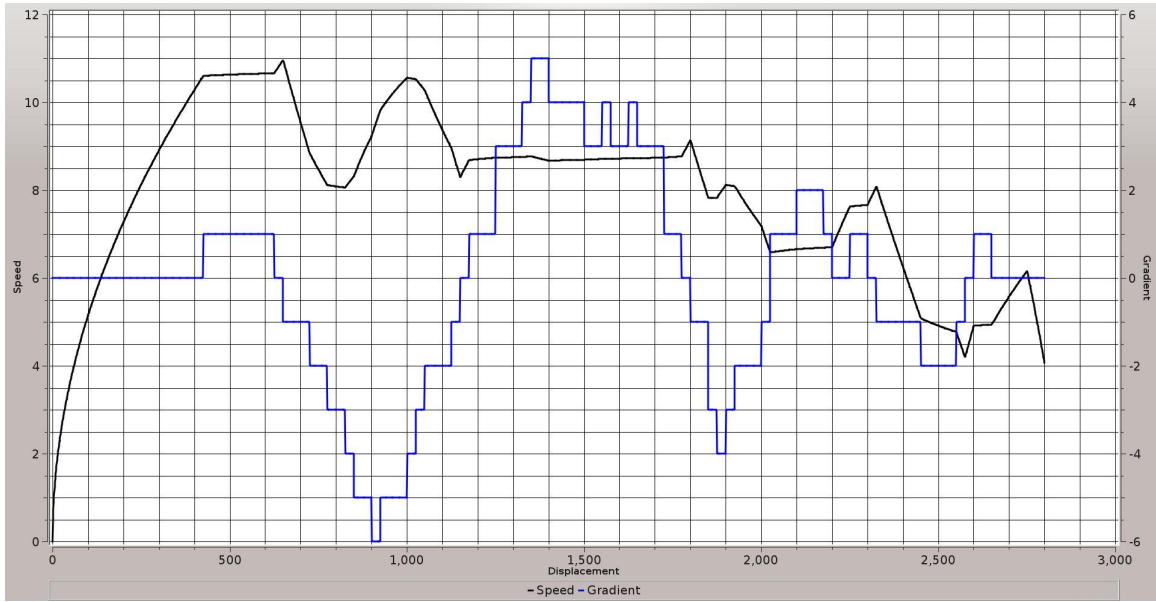


Figure 4.14: Graph of Speed and Gradient versus displacement for "Preset Strategy 3"

ous strategies' value to 34N.m which occurs at around 650m displacement due to the peak vehicle speed at that point. By implementing this strategy, the maximum air drag dropped by 35.2% .

Table 4.5 shows the main simulation result for "Preset Strategy 3". The total energy consumption is less than the previous strategies which is 216385J and the mileage increases to 46.6km/kWh. The lap time is increases to 390.491 seconds, hence the attempt time would be 1602 seconds which is equal to 26 mins and 42 seconds. The attempt time is slightly (1 minute and 18 seconds) under the time limit (28 minutes).

Result	Value
Total Energy Consumption	216385J
Total Time for 1 Lap	390.491s
Mileage	46.6 km/kWh

Table 4.5: Main result for "Preset Strategy 3"

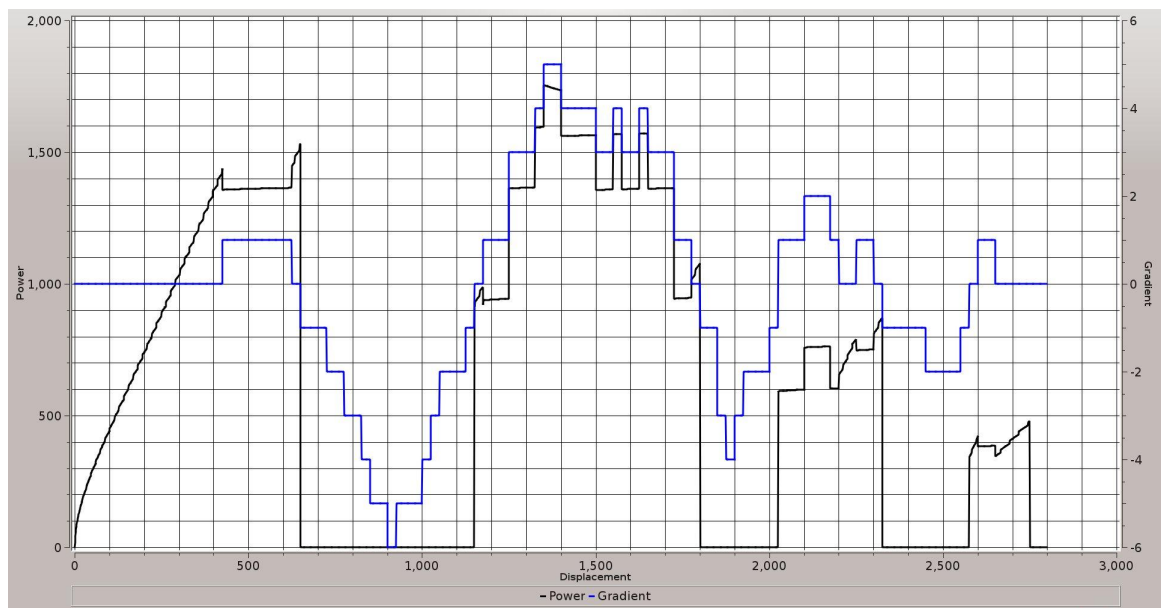


Figure 4.15: Graph of Power and Gradient versus displacement for "Preset Strategy 3"

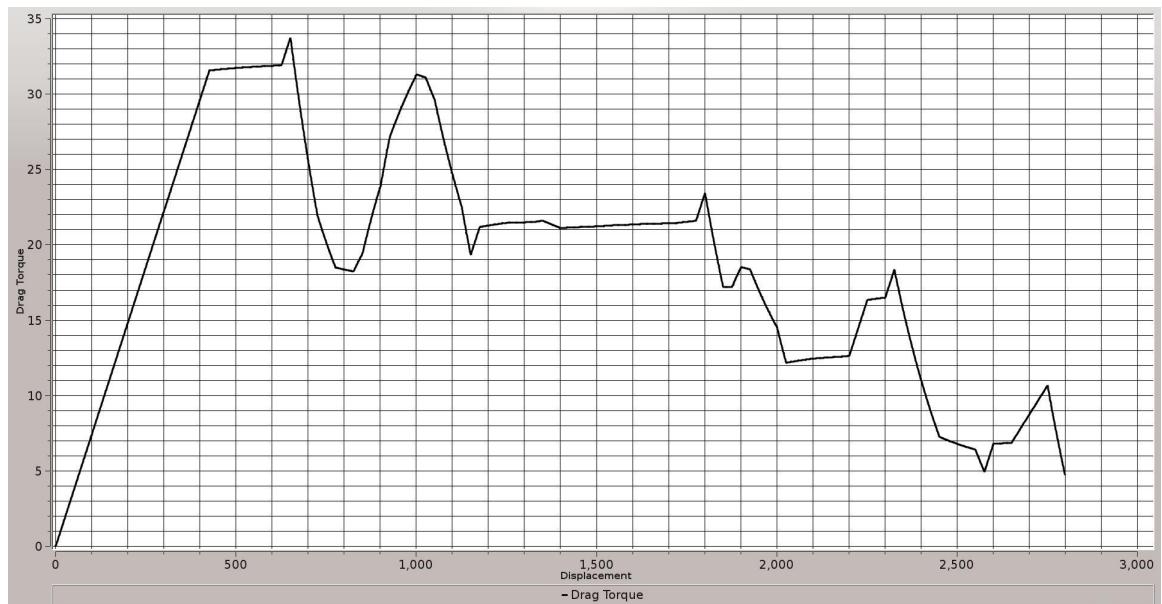


Figure 4.16: Graph of air drag versus displacement for "Preset Strategy 3"

4.5.4 Comparison Between Strategies

Figure 4.17 shows the power versus displacement curves for various strategies. As shown in the graph, the power output of the electric vehicle reduces from "Full Throttle Everywhere" strategy to "Preset Strategy 3". "Preset Strategy 1" and "Preset Strategy 2" shares some similarity because both of these strategies uses full throttle when the gradient is positive. Figure 4.18 is the histogram of the energy consumption of the 4 strategies while figure 4.19 is the mileage for the strategies. Again, both mileage and energy consumption improves for every new strategy. Figure 4.20 is the lap time comparison graph for various strategies and figure 4.21 is the air-drag comparison graph for 4 the different strategies. Due to the decrease in the overall speed, the lap time increases while at the same time the air-drag decreases, which contributes to decrease in power output from the electric vehicle.

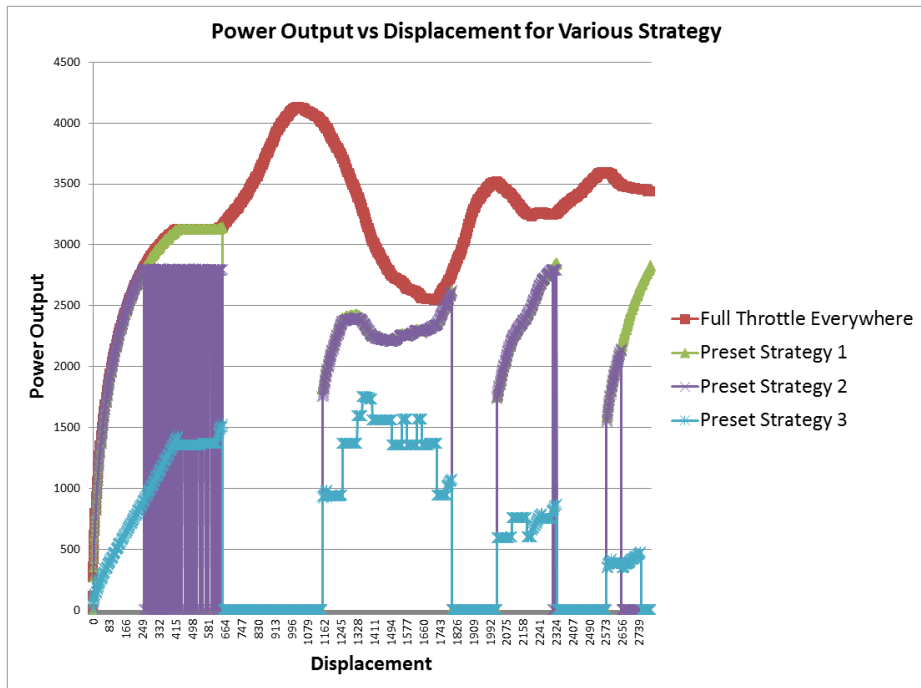


Figure 4.17: Graph of power output versus displacement for various strategy

Overall, by introducing optimize for Sepang North Track strategy which is the "Preset Strategy 3", the mileage of the electric vehicle improves from 18km/kWh to 46.58km/kWh which is a huge 158% increase in the mileage. Therefore, the weight of a good strategy is identified through the comparison between the strategies.

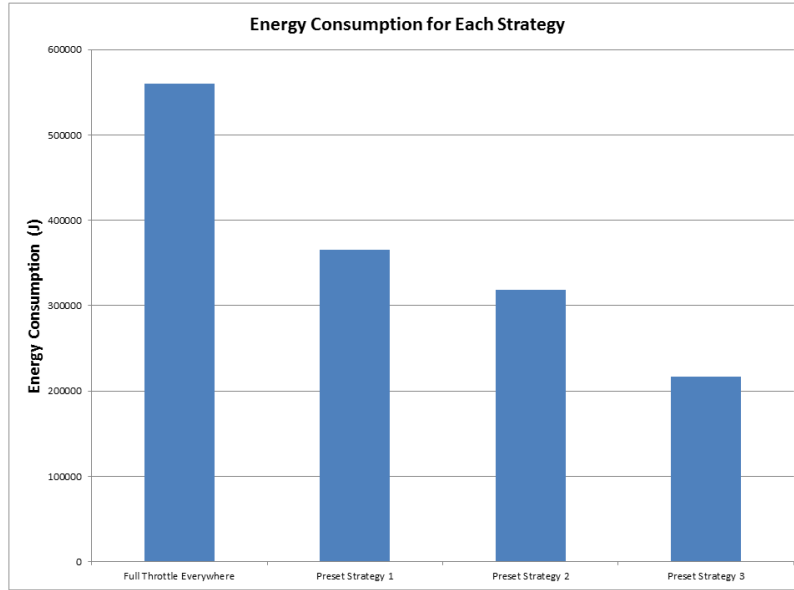


Figure 4.18: Graph of energy consumption for each strategy

Since this simulation software only simulates vehicle dynamics in ideal condition which is without wind, rain and air density at standard temperature and pressure, the power output of the electric vehicle at real life condition would be more than the simulated result for countering any other external forces acted on the vehicle. Apart from this, the overall efficiency of the electric vehicle is not included in this simulation, hence the real mileage of the electric vehicle would differ with the simulated mileage with a relationship shown in equation 4.1 where M_{real} is the real vehicle mileage, η is the overall efficiency of the electric vehicle and M_{sim} is the simulated vehicle mileage.

$$M_{real} = \eta M_{sim} \quad (4.1)$$

4.6 Summary

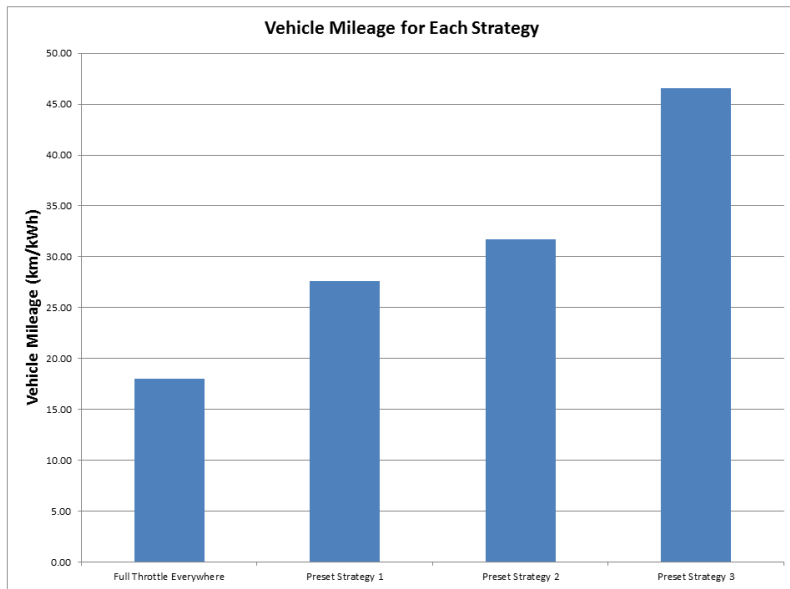


Figure 4.19: Graph of vehicle mileage for each strategy

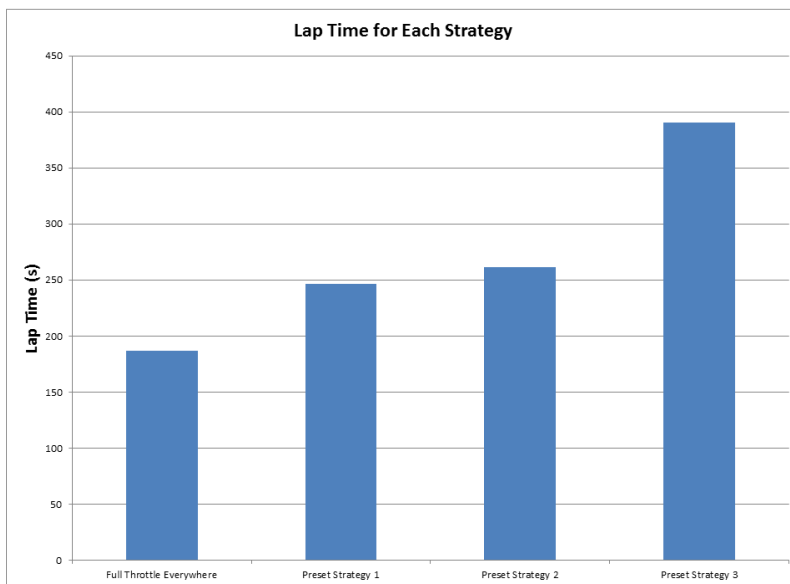


Figure 4.20: Graph of lap time for each strategy

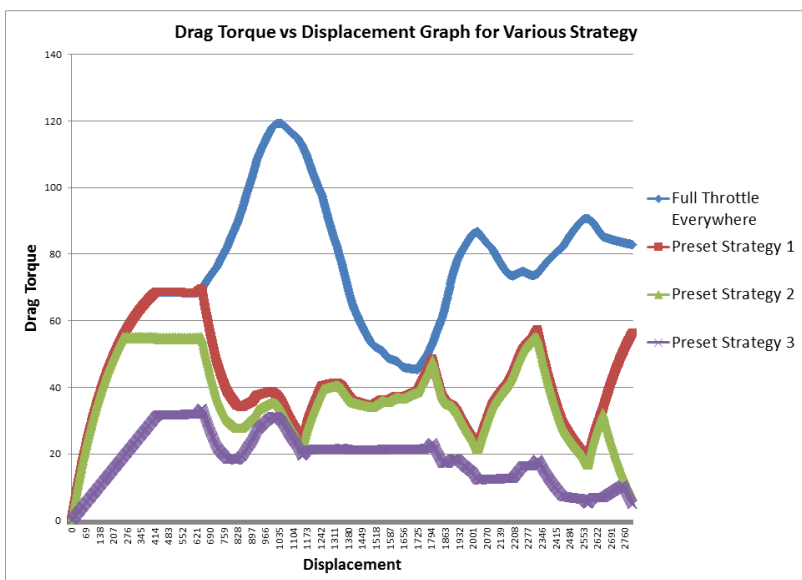


Figure 4.21: Graph of drag torque versus displacement for each strategy

CHAPTER 5

CONCLUSION

REFERENCES

- A., V. and N., D. (2011). Torque Ripple Minimization in Indirect Position Detection of Permanent Magnet Brushless DC Motor. *European Journal of Scientific Research*, 65(4):481–489.
- Bocharkov, Y., Tobias, A., Roberts, C., Hillmansen, S., and Goodman, C. (2007). Optimal Driving Strategy for Traction Energy Saving on DC Suburban Railways. *IET Electr. Power Appl.*, 19(5):675–682.
- Enany, M. A., Elshewy, H. M., and Abdel-kader, F. E. (2010). Brushless DC Motor Performance Improvement through Switch-on and Switch-off Angles Control. *Proceedings of the 14th International Middle East Power System Conference (MEPCON'10)*, pages 786–790.
- Howlett, P., Pudney, P., Tarnopolskaya, T., and Gates, D. (1997). Optimal Driving Strategy for a Solar Car on a Level Road. *IMA Journal of Mathematics Applied in Business & Industry*, pages 59–81.
- Jang, G. H. and Lee, C. J. (2006). Design and Control of the Phase Current of a Brushless DC Motor to Eliminate Cogging Torque. *Journal of Applied Physics*, page 3.
- Kim, T.-S., Ahn, S.-C., and Hyun, D.-S. (2001). A New Current Control Algorithm for Torque Ripple Reduction of BLDC Motors. *IECON'01: The 27th Annual Conference of the IEEE Industrial Electronics Society*, pages 521–526.
- Koot, M., Kessels, J. T. B. A., de Jager, B., Heemels, W. P. M. H., van den Bosch, P. P. J., and Steinbuch, M. (2005). Energy Management Strategies for Vehicular Electric Power Systems. *IEEE Transactions on Vehicular Technology*, 54(3):771–782.
- Nam, K.-Y., Lee, W.-T., Lee, C.-M., and Hong, J.-P. (2006). Reducing Torque Ripple of Brushless DC Motor by Varying Input Voltage. *IEEE Transactions on Magnetics*, 42(4):1307–1310.
- Park, S. J., Park, H. W., et al. (2000). A New Approach for Minimum-Torque-Ripple Maximum-Efficiency Control of BLDC Motor. *IEEE Transactions on Industrial Electronics*, 47(1):109–114.
- Parsa, L. and Hao, L. (2008). Interior Permanent Magenet Motors With Reduced Torque Pulsation. *IEEE Transactions on Industrial Electronics*, 55(2):602–609.
- Point, W. C. (1999). Understanding Hall Effect Sensors. http://www.wellsve.com/sft503/Counterpoint3_1.pdf.
- Pudney, P. and Howlett, P. (1994). Optimal Driving Strategies for a Train Journey with Speed Limits. *J. Austral. Math. Soc. Ser. B*, 36:38–49.

- Salah, W. A., Ishak, D., and Hammadi, K. J. (2011). PWM Switching Strategy For Torque Ripple Minimization in BLDC Motor. *Journal of Electrical Engineering*, 62(3):141–146.
- Shimizu, Y., Komatsu, Y., Torii, M., and Takamuro, M. (1998). Solar Car Cruising Strategy and Its Supporting System. *JSAE Review*, 19:143–149.
- Technologies, K. E. (2010). KLD D1064R Electric Drive System. <http://www.kldenergy.com/>.
- Yedamale, P. (2003). *Brushless DC (BLDC) Motor Fundamentals*. Microchip Technology Inc.

APPENDICES

APPENDIX A

SCHEMATIC